LETTER

Autophagy induction via STING trafficking is a primordial function of the cGAS pathway

Xiang Gui[1,3], Hui Yang[1,3], Tuo Li[1], Xiaojun Tan[1], Peiqing Shi[1], Minghao Li[1], Fenghe Du[1,2] & Zhijian J. Chen[1,2]*

Cyclic GMP-AMP (cGAMP) synthase (cGAS) detects infections or tissue damage by binding to microbial or self DNA in the cytoplasm[1]. Upon binding DNA, cGAS produces cGAMP that binds to and activates the adaptor protein STING, which then activates the kinases IKK and TBK1 to induce interferons and other cytokines[2–6]. Here we report that STING also activates autophagy through a mechanism that is independent of TBK1 activation and interferon induction. Upon binding cGAMP, STING translocates to the endoplasmic reticulum–Golgi intermediate compartment (ERGIC) and the Golgi in a process that is dependent on the COP-II complex and ARF GTPases. STING-containing ERGIC serves as a membrane source for LC3 lipidation, which is a key step in autophagosome biogenesis. cGAMP induced LC3 lipidation through a pathway that is dependent on WIPI2 and ATG5 but independent of the ULK and VPS34–beclin kinase complexes. Furthermore, we show that cGAMP-induced autophagy is important for the clearance of DNA and viruses in the cytosol. Interestingly, STING from the sea anemone *Nematostella vectensis* induces autophagy but not interferons in response to stimulation by cGAMP, which suggests that induction of autophagy is a primordial function of the cGAS–STING pathway.

To study DNA-induced autophagy, we transfected interferon-stimulatory DNA (ISD) into BJ cells, which are immortalized human fibroblasts. DNA transfection not only activated downstream components of the cGAS pathway such as STING, TBK1 and IRF3, but also stimulated conversion of LC3 into a lipidated form (LC3-II) (Extended Data Fig. 1a). By contrast, the synthetic double-stranded RNA analogue polyinosinic:polycytidylic acid (poly(I:C)) failed to stimulate LC3 lipidation despite stimulating phosphorylation of TBK1 and IRF3. Similarly, infection with the DNA virus herpes simplex virus-1 (HSV-1), but not the RNA virus Sendai virus, stimulated LC3 lipidation (Extended Data Fig. 1b). Furthermore, cGAMP delivery into BJ cells was sufficient to induce robust LC3 lipidation and STING degradation (Extended Data Fig. 1a), which was more prominent when the cells were pre-treated with chloroquine, which suggests an increase of the autophagy flux after cGAMP stimulation (Extended Data Fig. 1c). cGAMP-stimulated autophagosome formation was also visualized by LC3–GFP live cell imaging (Supplementary Video 1). Electron microscopy demonstrated that cGAMP induced the formation of double-membrane autophagosomes (Fig. 1a, b). Loss of cGAS blocked LC3 conversion triggered by herring testes DNA (HT-DNA) but not cGAMP, whereas loss of STING blocked LC3 conversion induced by both HT-DNA and cGAMP (Fig. 1c). Of interest, BJ cells deficient in TBK1 still retained LC3 lipidation in response to cGAMP treatment (Fig. 1d). Further experiments showed that STING vesicle trafficking, but not TBK1 phosphorylation of STING at Ser366, is required for cGAMP-induced autophagy (Extended Data Fig. 1d–l, Supplementary Videos 2, 3, Supplementary Information).

We next delineated the domains within STING required for autophagy induction. Deletion of the C-terminal activation domain (STING(1–340)) abolished phosphorylation of TBK1 and IRF3 but

did not impair LC3 conversion or STING degradation induced by cGAS or cGAMP. A mutation of a cGAMP-binding residue (R238A) in STING(1–340) blocked STING degradation and LC3 conversion (Fig. 1e). Further mapping identified a small region that spans residues
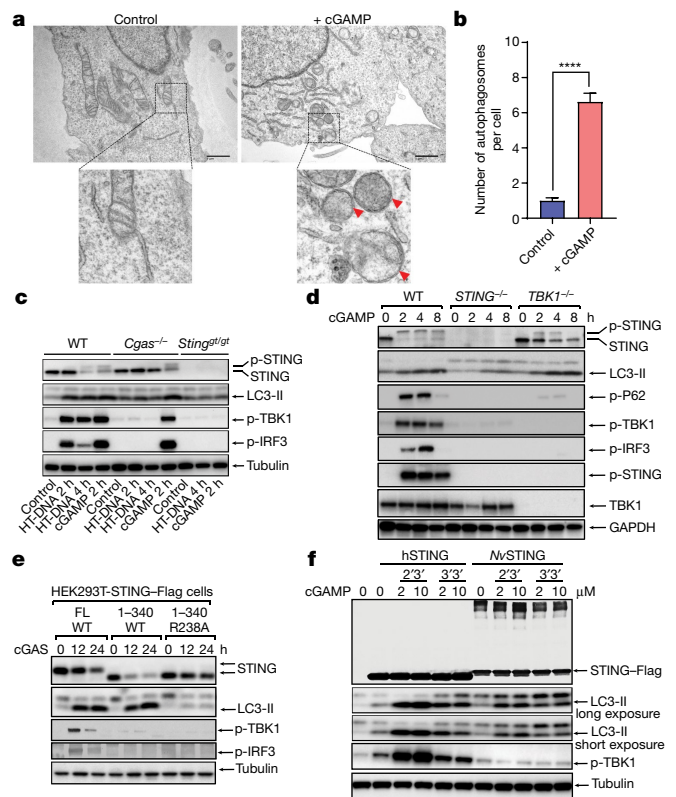
Fig. 1 | Autophagy induction by STING is evolutionarily conserved and separable from interferon induction. a, cGAMP induces autophagosome formation. Electron micrographs of BJ cells stimulated with cGAMP. Boxed areas are enlarged to show double-membrane organelles representing autophagosomes, as indicated by red arrowheads. **b**, The number of double-membrane autophagosomes per cell was obtained by counting BJ cells stimulated with ($n = 32$) or without cGAMP ($n = 39$). Means ± s.e.m. are shown. ****$P < 0.0001$ (two-tailed Student's *t*-test). **c**, DNA-induced LC3 lipidation requires cGAS and STING. Wild-type, $Cgas^{-/-}$ or $Sting^{gt/gt}$ primary MEF cells were stimulated with cGAMP or transfected with HT-DNA for the indicated time, followed by immunoblotting. WT, wild type. **d**, TBK1 is dispensable for LC3 conversion. Wild-type, $STING^{-/-}$ or $TBK1^{-/-}$ BJ cells were stimulated with cGAMP before cell lysates were analysed by immunoblotting. **e**, HEK293T cells that stably express the indicated STING proteins were transfected with a cGAS expression plasmid before cell lysates were analysed by immunoblotting. FL, full length. **f**, *Nv*STING stimulates LC3 conversion but not TBK1 activation. HEK293T cells expressing human STING (hSTING) or *Nv*STING were treated with indicated concentrations of 2′3′-cGAMP or 3′3′-cGAMP followed by immunoblotting.

[1]Department of Molecular Biology, Center for Inflammation Research, University of Texas Southwestern Medical Center, Dallas, Texas, USA. [2]Howard Hughes Medical Institute, University of Texas Southwestern Medical Center, Dallas, Texas, USA. [3]These authors contributed equally: X. Gui, H. Yang. *e-mail: Zhijian.Chen@UTSouthwestern.edu
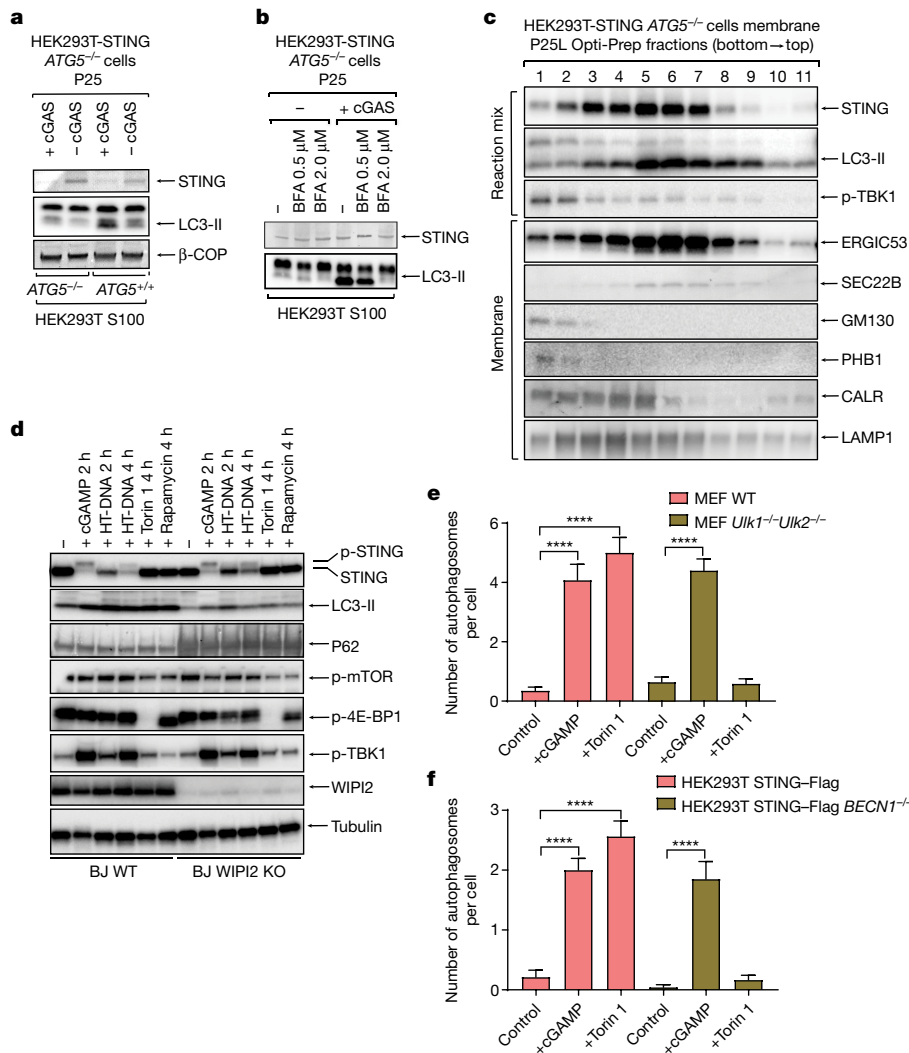
Fig. 2 | STING translocates to the ERGIC to trigger autophagosome formation. a, LC3 lipidation in vitro requires membranes from cGAS-stimulated cells and cytosolic extracts containing ATG5. *ATG5*−/− HEK293T cells that stably express STING were transfected with a cGAS expression plasmid for 18 h before membrane pellets (P25) were prepared by differential centrifugation. The membranes were incubated with cytosolic extracts (S100) from HEK293T cells followed by immunoblotting analysis. **b**, Membrane trafficking of STING is important for LC3 lipidation in vitro. Similar to **a** except that BFA was added to *ATG5*−/− HEK293T-STING cells at indicated concentrations before cells were transfected with a cGAS expression plasmid. **c**, ERGIC fractions are enriched with LC3 lipidation activity. Similar to **a** except that P25 membranes were further fractionated by Opti-Prep gradient ultracentrifugation. The reaction mixtures and each fraction from the ultracentrifugation were analysed by immunoblotting with the indicated antibodies. **d**, WIPI2 is required for STING-induced LC3 conversion. WIPI2-knockout (KO) BJ cells were treated with cGAMP, HT-DNA, torin 1 or rapamycin for the indicated time followed by immunoblotting of cell lysates. **e**, **f**, cGAMP induces autophagosome formation independently of ULK1 and BECN1. Wild-type and *Ulk1*−/−*Ulk2*−/− MEF cells (**e**), and HEK293T STING–Flag and HEK293T STING–Flag *BECN1*−/− cells (**f**) were stimulated with cGAMP or torin 1 as indicated. The number of double-membrane autophagosomes per cell was counted in MEF cells ($n = 17, 13, 13, 25, 20, 29$; left to right) or HEK293T-STING cells ($n = 14, 15, 16, 23, 20, 24$; left to right). Means ± s.e.m. are shown. ****$P < 0.0001$ (two-tailed Student's *t*-test).

330–334 of STING as important for autophagy induction (Extended Data Fig. 2a, b). Point mutations of residues within this region revealed that mutation of L333 and R334 to alanine within full-length STING abrogated LC3 conversion, phosphorylation of TBK1 and IRF3, and formation of STING and LC3 puncta induced by cGAMP (Extended Data Fig. 2c, d). The sequence surrounding this 'LR' motif is evolutionarily conserved (Extended Data Fig. 2e) and is found in the STING of *N. vectensis* (*Nv*STING), an anemone species that possesses a functional cGAS–STING pathway[7]. *Nv*STING does not contain the C-terminal domain required for activation of the type-I interferon pathway found in vertebrate STING (Extended Data Fig. 2e). *N. vectensis* cGAS (*Nv*cGAS) was reported to produce 3′3′-cGAMP[7]; however, we found that 2′3′-cGAMP stimulated stronger LC3 conversion than 3′3′-cGAMP in HEK293T cells that stably express human STING or *Nv*STING, but neither compound stimulated TBK1 activation through *Nv*STING (Fig. 1f). Truncated human STING(1–340)

mimicked *Nv*STING function after 2′3′-cGAMP stimulation in triggering LC3 lipidation without TBK1 or IRF3 phosphorylation (Extended Data Fig. 3a). Further experiments showed that *Nv*cGAS produces 2′3′-cGAMP rather than 3′3′-cGAMP (Extended Data Fig. 3b–d, Supplementary Information). STING from *Xenopus tropicalis* also lacks the C terminus required for TBK1 and IRF3 activation (Extended Data Fig. 3e). In response to 2′3′-cGAMP stimulation, *Xenopus* STING translocated from the endoplasmic reticulum and triggered LC3 conversion without activating TBK1 or IRF3 (Extended Data Fig. 3f–h). By contrast, STING from *Danio rerio*, which contains a C-terminal activation domain homologous to that of human STING, stimulated LC3 conversion as well as phosphorylation of TBK1 and IRF3 (Extended Data Fig. 3f–h). Taken together, our data show that the autophagy-inducing—but not the interferon-inducing function—of vertebrate STING is conserved in *Nematostella* and *Xenopus*, which suggests that autophagy induction is a primordial function of the cGAS–STING pathway.
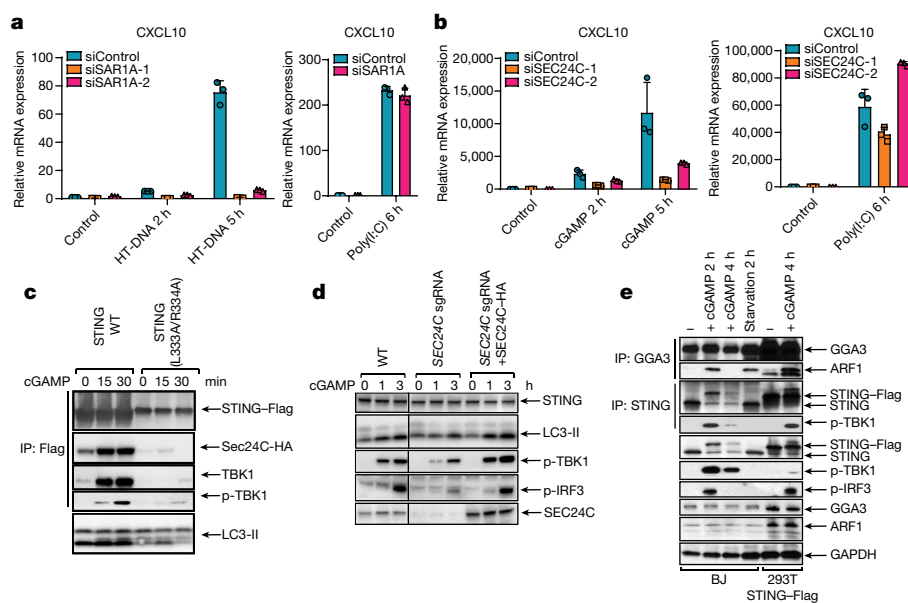
Fig. 3 | SAR1A and SEC24C are essential for STING trafficking and signalling. a, BJ cells were transfected with control siRNA (siControl) or siRNAs targeting *SAR1A* (siSAR1A-1 and siSAR1A-2) for three days before transfection with HT-DNA or poly(I:C) for the indicated time. Total RNA was isolated to measure the expression of indicated genes by reverse transcription qPCR. **b**, Similar to **a**, except HeLa cells were transfected with siRNAs targeting *SEC24C* (siSEC24C-1 and siSEC24C-2), and cells were stimulated with cGAMP or poly(I:C). Mean ± s.d. is shown. Data represent two independent experiments with three replicates. **c**, cGAMP induces STING binding to SEC24C. HEK293T cells that stably express SEC24C–HA and wild-type STING–Flag or the indicated STING mutant were stimulated with cGAMP before cell lysates were prepared for immunoprecipitation using anti-Flag antibody. Precipitated proteins were analysed by immunoblotting. **d**, SEC24C is required for LC3 lipidation and IRF3 phosphorylation. HEK293T cells that stably express STING were infected with lentiviruses containing *SEC24C* sgRNA to deplete endogenous SEC24C. To restore SEC24C expression, an aliquot of the cells was infected with lentiviruses expressing sgRNA-resistant *SEC24C* cDNA. The cells were stimulated with cGAMP followed by immunoblotting. **e**, cGAMP stimulates ARF1 GTPase activity. BJ and HEK293T-STING cells were treated with cGAMP or starved for the indicated time before cell lysates were immunoprecipitated with an antibody against GGA3 or STING, followed by immunoblotting with the indicated antibodies.

To investigate the mechanism by which STING activates autophagy, we examined STING trafficking using confocal microscopy. Upon cGAMP stimulation, STING first colocalized at the perinuclear region with ERGIC-53, a marker of the ERGIC, before colocalizing with LC3–GFP-positive autophagosomes (Extended Data Fig. 4a, Supplementary Video 4). STING trafficking to the ERGIC was also blocked by golgicide A (GCA; Extended Data Fig. 4b). These results are intriguing because recent studies have suggested that the ERGIC is a major source of membranes for starvation-induced LC3 lipidation[8]. To test whether the ERGIC serves as a membrane source for cGAMP-induced LC3 lipidation, we performed an in vitro reconstitution assay using cytosol (S100) from wild-type HEK293T cells and membranes (P25) from *ATG5*$^{-/-}$ HEK293T cells that stably express STING (*ATG5*$^{-/-}$ HEK293T-STING; Extended Data Fig. 4c). Consistent with a previous report[8], LC3 conversion was detected 1 h after membranes from *ATG5*$^{-/-}$ cells were incubated with cytosol from starved wild-type cells (Extended Data Fig. 4d). Importantly, LC3 conversion was detected when membranes from cGAS-stimulated *ATG5*$^{-/-}$ HEK293T-STING cells were incubated with cytosol from unstimulated wild-type cells (Fig. 2a, Extended Data Fig. 4d). By contrast, membranes from cGAS-stimulated cells treated with brefeldin A (BFA) lost the ability to stimulate LC3 conversion (Fig. 2b). These results suggest that vesicles budding from the endoplasmic reticulum and/or Golgi in cGAS-stimulated cells serve as the membrane source for LC3 conjugation by the cytosolic ATG5 conjugation machinery. To determine the types of vesicles that stimulate LC3 conjugation, we further fractionated the membranes from cGAS-stimulated *ATG5*$^{-/-}$ HEK293T-STING cells by differential centrifugation followed by sucrose gradient ultracentrifugation and Opti-Prep (iodixanol) density-gradient ultracentrifugation (Extended Data Fig. 4c). Each membrane fraction was incubated with the cytosolic extract from HEK293T cells to test for the ability to support LC3 conjugation (Fig. 2c, Extended Data Fig. 4e, f). This analysis revealed that membrane fractions enriched in STING and the ERGIC

markers ERGIC-53 and SEC22B had enhanced activity in stimulating LC3 conversion, which suggests that the ERGIC serves as a membrane source for LC3 conjugation. Additional experiments showed that STING traffics to lysosomes via autophagosomes and endosomes in a RAB7A-dependent manner (Extended Data Fig. 5, Supplementary Information).

We investigated the role of several autophagy-related genes in cGAMP-induced LC3 lipidation and STING degradation. ATG5 deficiency abolished LC3 lipidation but not STING degradation (Extended Data Fig. 6a). Basal levels of LC3 lipidation appeared to be higher in ATG9-deficient cells, but cGAMP-induced STING degradation was normal in these cells (Extended Data Fig. 6b). We next examined whether STING induces the inhibition of mTOR, which is known to regulate autophagy. mTOR and 4E-BP1 were dephosphorylated after treatment with the mTOR inhibitor torin 1 or rapamycin, but not after HT-DNA or cGAMP treatment, which triggered more robust LC3 conversion than the mTOR inhibitors (Extended Data Fig. 6c). WIPI2 is a phosphotidylinositol-3-phosphate (PI3P) effector protein that is important for LC3 lipidation in the conventional autophagy pathway[9]. We found that LC3 lipidation and P62 degradation were diminished in WIPI2-deficient cells after HT-DNA or cGAMP treatment, whereas TBK1 and IRF3 phosphorylation as well as STING degradation remained unaffected (Fig. 2d), which suggests that STING may induce LC3 conjugation through WIPI2. The kinases ULK1 and ULK2 are required for conventional autophagy induced by torin 1 (Fig. 2e, Extended Data Fig. 6d). Of interest, *Ulk1*$^{-/-}$*Ulk2*$^{-/-}$ mouse embryonic fibroblast (MEF) cells showed normal STING degradation, LC3 conversion and double-membrane autophagosome formation after HT-DNA transfection, cGAMP delivery or treatment with 5,6-dimethylxanthenone-4-acetic acid (DMXAA), which activates mouse STING (Fig. 2e, Extended Data Fig. 6e, f). Similarly, cGAMP-induced LC3 lipidation and autophagosome formation were normal in the absence of beclin 1, which is required for conventional autophagy
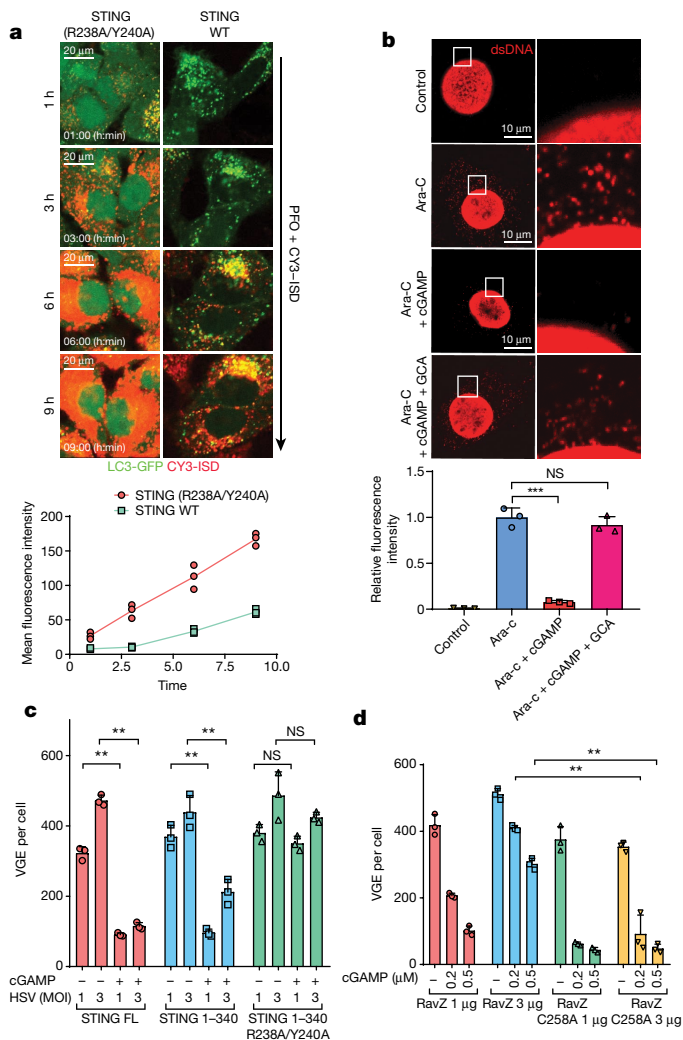
Fig. 4 | cGAMP-induced autophagy mediates the clearance of cytosolic DNA and DNA viruses. a, cGAMP binding by STING enhances the clearance of cytosolic DNA. Cy3–ISD was delivered into HeLa LC3–GFP cells that stably express wild-type STING or mutant STING(R238A/Y240A). Live cell imaging was carried out with still frames shown at the indicated times. Each mean fluorescence intensity of Cy3–ISD was calculated using ImageJ from three different areas, each of which contains three cells (bottom graph). $n = 3$. **b**, cGAMP enhances degradation of cytosolic DNA generated by DNA damage. MEF cells were treated with Ara-C for 12 h and then stimulated with cGAMP in the presence or absence of GCA for another 12 h. Cytosolic DNA was stained with a double-stranded-DNA-specific antibody. Intensity of cytosolic DNA staining was determined using ImageJ by deducting nuclear staining. Calculation was based on five cells from three different areas (bottom graph). Data are shown as mean ± s.e.m. ***$P < 0.001$ ($n = 3$, two-tailed Student's t-test); NS, not significant (significance level, $\alpha = 0.01$). **c**, Autophagy induction through STING(1–340) is sufficient to suppress HSV-1 replication. HEK293T cells that stably express wild-type or mutant STING were stimulated with cGAMP and then infected with HSV-1(ΔICP34.5) for 12 h at a multiplicity of infection (MOI) of 1 or 3. Viral DNA in the infected cells was quantified by qPCR using primers targeting the HSV-1 genome. VGE, virus genome equivalent. Mean ± s.d. is shown. Data represent two independent experiments with three replicates. $n = 3$. NS, not significant, two-tailed Student's t-test. **d**, LC3 deconjugation by RavZ abrogates the anti-viral effects of cGAMP. HEK293T-STING stable cells transiently expressing wild-type or RavZ(C258A) were stimulated with indicated concentrations of cGAMP before infection by HSV-1(ΔICP34.5) for 8 h. Viral DNA in infected cells was measured by qPCR to calculate virus genome equivalent. Data are presented as mean ± s.d. **$P < 0.01$ ($n = 3$, two-tailed Student's t-test).

(Fig. 2f, Extended Data Fig. 7, Supplementary Information). These results suggest that STING-containing ERGIC vesicles may activate LC3 lipidation through a WIPI2- and ATG5-dependent mechanism that is distinct from conventional autophagy.

Trafficking of proteins from the membrane and lumen of the endoplasmic reticulum is initiated by the budding of vesicles that requires the GTPase SAR1A and the COP-II complex that includes SEC24[10,11]. We found that knockdown of SAR1A or SEC24C expression in HeLa cells by small interfering RNA (siRNA) blocked STING puncta formation induced by cGAMP (Extended Data Fig. 8a, b). Depletion of each protein also inhibited induction of IFNβ and the chemokine CXCL10 by DNA or cGAMP but not by poly(I:C) (Fig. 3a, b, Extended Data Fig. 8c, d). Co-immunoprecipitation experiments showed that cGAMP induced the interaction between STING and SEC24C at early time points and that this interaction was disrupted by mutating L333 and R334 on STING (Fig. 3c). We then used the CRISPR technology to knock out SEC24C in HEK293T-STING cells; a single-guide RNA (sgRNA) against *SEC24C* was efficient in nearly depleting endogenous SEC24C without single-cell cloning (Fig. 3d). Depletion of SEC24C inhibited LC3 conversion and phosphorylation of TBK1 and IRF3; the residual activity may be due to the presence of some wild-type cells in the pool. When the knockout cells were rescued with SEC24C, the cGAMP signalling pathway was fully restored (Fig. 3d). These results indicate that the formation of the COP-II vesicle is important for the signalling events downstream of cGAMP binding to STING. We further showed that cGAMP stimulation enhanced the binding of the GTPase ARF1—which regulates vesicle trafficking[10,12]—to its effector protein GGA3 (Fig. 3e), indicating that cGAMP activates ARF1. Inhibition or depletion of ARF1 strongly suppressed the signalling cascade induced by DNA but not RNA (Extended Data Fig. 8e–i, Supplementary Information).

Our findings that the autophagy-inducing activity of STING pre-dates its interferon-inducing activity during evolution raises the question of the role of autophagy induction by the cGAS–STING pathway. We first examined whether autophagy induction by cytosolic DNA provides a mechanism for DNA clearance from the cytosol. Cy3–ISD activated endogenous cGAS to produce cGAMP, which led to LC3 puncta formation in STING-expressing but not STING-deficient cells (Extended Data Fig. 9a). Colocalization of LC3 puncta with Cy3–ISD was evident in cells that express wild-type STING but not in cells that express mutant STING(R238A/Y240A) (Fig. 4a, Extended Data Fig. 9a), suggesting DNA was targeted by STING-induced autophagy. Live cell imaging showed that Cy3–ISD was enclosed by the LC3 puncta (Supplementary Video 5) and cGAMP delivery further accelerated LC3 puncta formation and DNA degradation (Supplementary Video 6). These results indicate that cGAMP-induced autophagy facilitates the clearance of cytosolic DNA. To investigate whether cGAMP enhances the clearance of endogenous DNA, we used arabinofuranosyl cytidine (Ara-C), which causes DNA damage by interfering with DNA synthesis. Ara-C treatments led to accumulation of DNA in the cytosol (Fig. 4b). cGAMP treatment resulted in the disappearance of cytosolic DNA, an effect that was blocked by GCA (Fig. 4b). We further tested whether cGAMP-induced autophagy is important for host defence against viruses. Quantitative PCR (qPCR) measurement of the viral genome equivalents revealed that cells that express full-length STING or STING(1–340), but not STING(1–340) with the cGAMP binding mutations R238A/Y240A, had reduced HSV-1 titre in response to cGAMP treatment (Fig. 4c). Similarly, fluorescence-activated cell sorting analyses showed that the titres of HIV–GFP (Extended Data Fig. 9b) and HSV–GFP virus (Extended Data Fig. 9c) were significantly lower in cGAMP-stimulated HEK293T cells that express full-length STING or STING(1–340) but not the STING(1-340, R238A/Y240A) mutant. STING(1–340) did not induce IFNβ or TNF in response to cGAMP delivery, confirming that the antiviral effect of this STING mutant is independent of cytokine induction (Extended Data Fig. 9d). To further evaluate the role of autophagy in antiviral defence, we employed the *Legionella* protein RavZ, an enzyme that irreversibly

cleaves LC3 from phosphatidylethanolamine on the membrane[13]. Wild-type RavZ expression in HEK293T-STING cells removed LC3 conjugation (Extended Data Fig. 9e) and largely prevented the inhibitory effect of cGAMP on HSV-1 replication (Fig. 4d); the residual inhibitory effect of cGAMP may be due to induction of interferons and other antiviral cytokines. By contrast, a catalytically inactive mutant, RavZ(C258A), did not interfere with the inhibition of HSV-1 replication by cGAMP (Fig. 4d, Extended Data Fig. 9e). Knocking out ATG5 but not TBK1 or BECN1 largely abrogated the inhibitory effect of cGAMP on HSV-1 as measured by HSV–GFP fluorescence intensity and normalized virus titre (Extended Data Fig. 9f, g). Taken together, these results indicate that cGAMP-induced autophagy has a crucial role in antiviral defence.

A unique and important feature of the cGAS–STING pathway is the robust activation of autophagy in addition to induction of interferons and inflammatory cytokines. cGAMP-induced LC3 lipidation is independent of TBK1 and the C-terminal signalling domain of STING, which is required for type-I interferon induction[14,15]. Conversely, activation of TBK1 and IRF3 remains intact in ATG5-deficient cells that are defective in LC3 lipidation and autophagosome formation. Thus, the autophagy- and interferon-inducing activities of STING can be uncoupled. After cGAMP binds to STING, STING interacts with SEC24C and buds from the endoplasmic reticulum into COP-II vesicles, which then form the ERGIC (Extended Data Fig. 10). The ERGIC serves as the membrane source for WIPI2 recruitment and LC3 lipidation, leading to formation of autophagosomes that target cytosolic DNA or DNA viruses for degradation by the lysosome. A fraction of STING traffics from the ERGIC to the Golgi network and post-Golgi vesicles such as late endosomes, at which STING activates TBK1 and IRF3, leading to induction of type-I interferon. STING in the autophagosomes and endosomes continues to traffic to the lysosome where it is degraded in a RAB7-dependent manner (Extended Data Fig. 10). Of note, the sea anemone, which belongs to a clade that diverged from that of *Homo sapiens* more than 500 million years ago, possesses a STING homologue (*Nv*STING) that lacks the C-terminal TBK1 activation domain[7]; nevertheless, *Nv*STING is still capable of stimulating LC3 conversion in response to cGAMP. Thus, autophagy induction is an ancient and highly conserved function of the cGAS–STING pathway that pre-dates the emergence of the type-I interferon pathway in vertebrates.

Online content

Any methods, additional references, Nature Research reporting summaries, source data, statements of data availability and associated accession codes are available at https://doi.org/10.1038/s41586-019-1006-9.

1. Sun, L., Wu, J., Du, F., Chen, X. & Chen, Z. J. Cyclic GMP-AMP synthase is a cytosolic DNA sensor that activates the type I interferon pathway. *Science* **339**, 786–791 (2013).
2. Wu, J. et al. Cyclic GMP-AMP is an endogenous second messenger in innate immune signaling by cytosolic DNA. *Science* **339**, 826–830 (2013).
3. Ishikawa, H. & Barber, G. N. STING is an endoplasmic reticulum adaptor that facilitates innate immune signalling. *Nature* **455**, 674–678 (2008).
4. Wu, J. & Chen, Z. J. Innate immune sensing and signaling of cytosolic nucleic acids. *Annu. Rev. Immunol*. **32**, 461–488 (2014).
5. Zhong, B. et al. The adaptor protein MITA links virus-sensing receptors to IRF3 transcription factor activation. *Immunity* **29**, 538–550 (2008).
6. Crowl, J. T., Gray, E. E., Pestal, K., Volkman, H. E. & Stetson, D. B. Intracellular nucleic acid detection in autoimmunity. *Annu. Rev. Immunol*. **35**, 313–336 (2017).
7. Kranzusch, P. J. et al. Ancient origin of cGAS–STING reveals mechanism of universal 2′,3′ cGAMP signaling. *Mol. Cell* **59**, 891–903 (2015).
8. Ge, L., Melville, D., Zhang, M. & Schekman, R. The ER-Golgi intermediate compartment is a key membrane source for the LC3 lipidation step of autophagosome biogenesis. *eLife* **2**, e00947 (2013).
9. Dooley, H. C. et al. WIPI2 links LC3 conjugation with PI3P, autophagosome formation, and pathogen clearance by recruiting Atg12-5-16L1. *Mol. Cell* **55**, 238–252 (2014).
10. Brandizzi, F. & Barlowe, C. Organization of the ER-Golgi interface for membrane traffic control. *Nat. Rev. Mol. Cell Biol*. **14**, 382–392 (2013).
11. Ge, L., Baskaran, S., Schekman, R. & Hurley, J. H. The protein–vesicle network of autophagy. *Curr. Opin. Cell Biol*. **29**, 18–24 (2014).
12. D'Souza-Schorey, C. & Chavrier, P. ARF proteins: roles in membrane traffic and beyond. *Nat. Rev. Mol. Cell Biol*. **7**, 347–358 (2006).
13. Choy, A. et al. The *Legionella* effector RavZ inhibits host autophagy through irreversible Atg8 deconjugation. *Science* **338**, 1072–1076 (2012).
14. Tanaka, Y. & Chen, Z. J. STING specifies IRF3 phosphorylation by TBK1 in the cytosolic DNA signaling pathway. *Sci. Signal*. **5**, ra20 (2012).
15. Liu, S. et al. Phosphorylation of innate immune adaptor proteins MAVS, STING, and TRIF induces IRF3 activation. *Science* **347**, aaa2630 (2015).

Author contributions X.G. and H.Y. planned the study under the guidance of Z.J.C., performed all experiments, and analysed the data. T.L. performed the mass spectrometry experiments. P.S. and F.D. generated several cell lines used in this study. Z.J.C. designed and supervised this study. X.G., H.Y., X.T., M.L. and Z.J.C. prepared and revised the manuscript.

METHODS

Data reporting. No statistical methods were used to predetermine sample size. The experiments were not randomized and the investigators were not blinded to allocation during experiments and outcome assessment.

Reagents and general methods. 2′3′-cGAMP was synthesized as previously described[16]. Poly(I:C), HT-DNA, Ara-C and aphidicolin were from Sigma-Aldrich. ISD and Cy3–ISD were prepared from equimolar amounts of sense and antisense DNA oligonucleotide (sense: 5′-TACAGATCTACTAGTGATCTATG-3′; anti-sense: 5′-ACTGATCTGTACATGATCTACA-3′). The oligonucleotides, synthesized at Sigma-Aldrich, were heated at 95 °C for 5 min and cooled to room temperature. BFA, GCA, BX-795, TPCA-1, MG132 and Velcade were purchased from Selleckchem; bafilomycin A1 and chloroquine were from Invivogen. siRNA oligonucleotides were purchased from Sigma and transfected into cells using Lipofectamine RNAiMAX (Thermo Fisher Scientific). The sense strand sequences are shown in Supplementary Table 1.

The procedures for IRF3 dimerization assay, sodium dodecyl sulfate polyacrylamide gel electrophoresis (SDS–PAGE), western blotting and immunoprecipitation have previously been described[17]. cGAMP was delivered into cells by permeabilization with digitonin (10 μg ml^{-1}) for 15 min in buffer A (50 mM HEPES-KOH, pH 7.2, 100 mM KCl, 3 mM MgCl$_2$, 0.1 mM DTT, 85 mM Sucrose, 0.2% BSA, 1 mM ATP). The concentration of cGAMP used in stimulating BJ cells was 0.2 μM or 0.5 μM unless indicated otherwise. ISD, HT-DNA, and poly(I:C) were transfected into cells using Lipofectamine 2000 (Thermo Fisher) at a concentration of 2 μg ml^{-1}. Cy3–ISD (1 μg ml^{-1}) was delivered into cells by permeabilization with perfringolysin O (PFO; 0.1 μg ml^{-1}). A 1-h pre-treatment was used for all inhibitors before DNA transfection or cGAMP stimulation at the following concentrations: BFA, 2 μM; bafilomycin A1, 0.2 μM; chloroquine, 20 μM; MG132, 10 μM; Velcade, 2 μM; GCA, 10 μM.

Antibodies. Rabbit antibodies against human STING, p-IRF3(Ser396), p-TB-K1(Ser172), p-IKKβ(Ser177), ATG5, ATG9, beclin1, calreticulin and GAPDH were from Cell Signaling. Rabbit Polyclonal antibody against mouse STING was from Proteintech. Mouse antibody against STING was purchased from R&D Systems; rabbit antibodies against human IRF3, TGN38 and ARF1, and mouse antibody against CD63 were from Santa Cruz Biotechnology; rabbit antibody against LC3 was from Novus Biologicals; mouse antibodies against P62 and GGA3 were from BD Transduction Laboratories; mouse antibody against ERGIC-53 was from Axxora; rabbit antibody against SEC22B was from Synaptic Systems; mouse antibody against Flag tag, rabbit antibodies against ERGIC53 and β-tubulin, anti-Flag (M2)-conjugated agarose and anti-HA-conjugated agarose were from Sigma; HA antibodies were from Covance; rabbit antibodies against GBF1, LAMP2 and giantin were from Abcam; rabbit antibody against beta-COP was from Thermo Fisher; rabbit antibodies against ARFGEF1, ARFGEF2 and SEC24C were from Bethyl Laboratories.

Expression constructs, viruses, cells and transfection. For transient expression in mammalian cells, human cDNAs encoding N-terminal tagged cGAS and C-terminal tagged STING were cloned into pcDNA3. For stable expression in mammalian cells, human cDNAs encoding C-terminal Flag-tagged STING and its mutants were cloned into a pTY-EF1A-IRES lentiviral vector[15], which was modified from PTY-shRNA-EF1a-puroR-2a-Flag provided by Y. Zhang (Harvard Medical School). These lentiviruses were packaged in HEK293T cells and transduced into target cells as previously described[14]. STING mutants were constructed using the QuikChange Site-Directed Mutagenesis Kit. Plasmids for mammalian expression of wild-type and C258A RavZ were provided by C. Roy (Yale). Plasmids and HT-DNA were transfected into cells using Lipofectamine 2000 (Life Technologies).

All cells were cultured at 37 °C in an atmosphere of 5% (v/v) CO$_2$. HEK293T and HeLa cells were cultured in Dulbecco's modified Eagle's medium (DMEM) supplemented with 10% (v/v) cosmic calf serum (Hyclone), penicillin (100 U ml^{-1}) and streptomycin (100 μg ml^{-1}). MEF, L929, Vero and BJ-hTERT cells were cultured in DMEM supplemented with 10% (v/v) fetal bovine serum (FBS, Atlanta) and antibiotics. THP1 cells were cultured in RPMI 1640 supplemented with 10% FBS, 2 mM β-mercaptoethanol and antibiotics. HeLa cells that stably express LC3–GFP and mouse bone marrows containing macrophages deficient in beclin 1 were provided by B. Levine (UT Southwestern). Ulk1$^{-/-}$ Ulk2$^{-/-}$ double-knockout MEF cells were from Sigma (14050803-1VL). To induce autophagy by starvation, cells were washed with PBS three times and cultured in Earles Balanced Salt Solution (EBSS).

Sendai virus (Cantell strain, Charles River Laboratories) was used at a final concentration of 50 haemagglutinating units per ml. HSV-1 wild-type strain was propagated and titred by plaque assays on Vero Cells and used at the indicated multiplicity of infection in BJ cells. The HSV-1(ΔICP34.5) strain was used at the indicated multiplicity of infection in BJ and HEK293T cells. Plasmids for HIV-GFP and VSV-G have previously been described[18]; HIV–GFP lentiviral plasmid was co-transfected with the VSV-G plasmid into HEK293T cells for virus packaging. Supernatants containing the viruses were collected, filtered and concentrated by PEG8000 precipitation. The titres of HIV–GFP virus were measured by infecting

HEK293T cells and performing flow cytometry analysis of GFP$^+$ cells 24 h after infection in the presence of 10 μg ml^{-1} polybrene. HSV1-GFP was provided by A. Iwasaki (Yale).

Generation of knockout cells by CRISPR–Cas9. Single-guide RNAs (sgRNA) were designed to target the human *CGAS*, *STING* (also known as *TMEM173*), *TBK1*, *ARF1*, *GBF1*, *ATG5*, *ATG9*, *ULK1*, *BECN1* and *SEC24C* genomic loci (Supplementary Table 2). The sgRNA sequence driven by a U6 promoter was cloned into a lentiCRISPR vector that also expresses Cas9 as previously described[19]. The lentiviral plasmid DNA was then packaged into a lentivirus for infection in HEK293T cells or BJ cells. Infected cells were selected in puromycin (2 μg ml^{-1}) for two weeks before single colonies were chosen and tested by immunoblotting, TA cloning and DNA sequencing.

Generation of primary mouse embryonic fibroblasts and bone-marrow-derived macrophages. *Cgas*$^{-/-}$ mice were generated as previously described[20]. *Sting*$^{gt/gt}$ mice were from the Jackson laboratory[21]. These strains were maintained on a C57BL/6J background. MEFs were generated from E13.5 embryos of wild-type and mutant mice under normal culture conditions[22]. Fresh leg bones from LysM-Cre$^+$*Becn1*$^{fl/fl}$ and *Becn1*$^{fl/fl}$ mice were provided by B. Levine (UT Southwestern). Bone-marrow-derived macrophages were generated as previously described[20]. All mice were bred and maintained under specific pathogen-free conditions in the animal care facility of University of Texas Southwestern Medical Center at Dallas according to experimental protocols approved by the Institutional Animal Care and Use Committee.

Immunostaining, confocal microscopy and live cell imaging. For immunostaining, cells were fixed with 4% paraformaldehyde, permeabilized with Triton X100 (0.2%) and stained with a primary antibody followed by a fluorescent secondary antibody. Nuclei were labelled by staining with DAPI in the mounting medium (Vectashield). Images of cells were collected with a Zeiss LSM710 META laser scanning confocal microscope and processed using Zeiss LSM image browser. In some experiments, images were collected with a Nikon A1R confocal microscope and processed using ImageJ. For live cell imaging, cells were grown on a four-chambered cover glass (Laboratory-Tek II, 155382) at a density of 40,000 cells per chamber (around 50% confluency) in 5% CO$_2$ and 20% O$_2$ at 37 °C, and videos were recorded using Nikon A1R confocal laser microscope system and further processed and analysed using ImageJ.

Flow cytometry. After HIV–GFP or HSV–GFP infection, cells were washed in fluorescence-activated cell sorting (FACS) buffer (PBS, 1% BSA), fixed with 2% paraformaldehyde, and analysed on BD FACS Calibur (BD Biosciences). Data analysis was performed using FlowJo software.

Electron microscopy. BJ cells were grown on glass-bottom plates before stimulation with cGAMP (0.2 μM for BJ cells and 1 μM for MEF cells and HEK293T cells) or torin 1 (1 μM for all cells). Samples were fixed, sectioned, stained and coated by the UTSW Electron Microscopy core facility. The images were visualized using FEI Tecnai transmission electron microscopes.

Reverse transcription qPCR and HSV1 genome qPCR. Reverse transcription quantitative PCR (RT–qPCR) reactions were carried out using the iScript cDNA synthesis kit and iQ SYBR Green Supermix (Bio-Rad). qPCR was performed on an Applied Biosystems Vii7 using the primers shown in Supplementary Table 1. HSV-1-infected cells were washed and lysed in a buffer containing 1% SDS, 50 mM Tris-CL (pH 7.5) and 10 mM EDTA, and the cell extract was incubated with proteinase K (2 mg ml^{-1}) at 37 °C for 30 min. DNA was extracted by phenol/chloroform extraction and ethanol precipitation. Viral DNA was quantified by qPCR using three different pair of primers corresponding to distinct regions of the HSV-1 genome (Supplementary Table 3).

In vitro LC3 lipidation assay. The in vitro LC3 assay was modified from published methods[8]. Cytoplasmic extract (S100) was prepared from wild-type or *ATG5*$^{-/-}$ HEK293T cells grown in normal or EBSS starvation medium for 2 h. After washing with PBS, cells were lysed by passing through a 25 G needle in a 3× cell pellet volume of hypotonic buffer (20 mM HEPES-KOH, pH 7.2, 10 mM KCl, 3 mM MgCl$_2$) plus cocktail protease inhibitors and phosphatase inhibitors (Roche). The cell lysate was centrifuged at 100,000g for 2 h to collect the S100 supernatant. For P25 membrane preparation, *ATG5*$^{-/-}$ HEK293T-STING cells were either left untreated or transfected with a cGAS expression plasmid for 12 h. Then, cells were washed with PBS and homogenized by douncing for 20 times in a buffer (20 mM HEPES-KOH, 400 mM sucrose, 0.5 mM EDTA). The homogenate was centrifuged at 1,000g for 5 min to remove cell debris and nuclei. The supernatant (S1) was further centrifuged at 5,000g for 10 min to precipitate mitochondria and other heavy organelles (P5). The supernatant (S5) was further centrifuged at 25,000g for 30 min to pellet membranes (P25). For each reaction, S100 (2 mg ml^{-1} final concentration), ATP regeneration system (40 mM creatine phosphate, 0.2 mg ml^{-1} creatine phosphokinase, and 1 mM ATP), GTP (0.15 mM), and P25 or different membrane fractions (0.2 mg ml^{-1}) were incubated in a final volume of 30 μl. The mixture was incubated at 30 °C for the indicated time followed by SDS–PAGE and immunoblotting.

Membrane fractionation. *Differential centrifugation of membranes.* Cells (five 15-cm dishes) were cultured to confluence, collected and homogenized by passing through a 25 G needle ten times in a 5× cell pellet volume of hypotonic buffer. Homogenates were subjected to sequential centrifugation at 1,000*g* (10 min), 5,000*g* (10 min), 25,000*g* (20 min) and 100,000*g* (30 min) to collect the P1, P5, P25 and P100 membranes, respectively. Membrane fractions containing equal amounts of proteins were used for the LC3 lipidation assay as described above.

Sucrose gradient ultracentrifugation. The P25 membrane fraction, which contained the highest LC3 lipidation activity, was used to purify ERGIC- and Golgi-containing fractions using a Golgi isolation kit (Sigma). The P25 membranes were suspended in 0.75 ml of 1.25 M sucrose buffer and overlaid first with 0.5 ml of 1.1 M and then with 0.5 ml of 0.25 M sucrose buffer and centrifuged at 120,000*g* for 3 h. The P25 L fraction at the interface between the 0.25 M and 1.1 M sucrose layers and the pellet on the bottom (P25 P fraction) were used to test LC3 lipidation activity.

Opti-Prep gradient ultracentrifugation. The P25 L fraction was suspended in 1 ml 19% Opti-Prep for the following Opti-Prep step gradient from bottom to top: 0.33 ml 22.5%, 0.66 ml 19% (sample), 0.6 ml 16%, 0.6 ml 12%, 0.66 ml 8%, 0.33 ml 5%, and 0.14 ml 0%. Each density of Opti-Prep was prepared by diluting 50% Opti-Prep (20 mM Tricine-KOH, pH 7.4, 42 mM sucrose and 1 mM EDTA) with a buffer of 20 mM Tricine-KOH, pH 7.4, 250 mM sucrose, and 1 mM EDTA. The Opti-Prep gradient was formed by centrifugation using a SW60 Swinging bucket Ti Rotor at 150,000*g* for 3 h with 10 fractions collected from the top to bottom. Fractions were diluted with hypotonic buffer and membranes were collected by centrifugation at 100,000*g* for 1 h. The activity of each fraction was tested as previously described[8].

cGAMP detection by mass spectrometry. HEK293T cells were transfected with expression plasmids encoding cGAS, a dinucleotide cyclase from *Vibrio cholerae* (DncV) or *Nvc*GAS. Small molecules were extracted from cells as previously described[23]. In brief, cells were lysed in 80% methanol and 2% acetic acid solution before the addition of an internal standard and an equal volume of 2% acetic acid. Insoluble fractions were pelleted by centrifugation and were extracted two more times in 2% acetic acid. After combining all three extracts, cyclic dinucleotides were enriched by solid-phase extraction on a Hypersep NH2 column (Thermo), washed with 2% acetic acid and with 80% methanol, and eluted with 20% ammonium hydroxide in methanol. After drying by vacuum centrifugation, samples were reconstituted in water and analysed by a Dionex U3000 HPLC coupled with a TSQ Quantiva Triple Quandrupole mass spectrometer. Data were collected by product ion scans that target an *m/z* of 675, and analysed with XCalibur (Thermo).

Statistics and reproducibility. Representative results from at least two independent repeats are shown for every figure, except where specified otherwise in the figure legends.

Data are shown as the mean ± s.e.m. unless indicated otherwise. GraphPad Prism 8 software (GraphPad) was applied for statistical analysis. For comparisons between two groups, the Student's *t*-test (unpaired and two-tailed) was applied.

Reporting summary. Further information on research design is available in the Nature Research Reporting Summary linked to this paper.

Data availability

The authors declare that all relevant data supporting the findings of this study are available within the paper and its supplementary information files. Additional information including raw data are available from the corresponding author upon reasonable request.

16. Zhang, X. et al. Cyclic GMP–AMP containing mixed phosphodiester linkages is an endogenous high-affinity ligand for STING. *Mol. Cell* **51**, 226–235 (2013).
17. Seth, R. B., Sun, L., Ea, C. K. & Chen, Z. J. Identification and characterization of MAVS, a mitochondrial antiviral signaling protein that activates NF-κB and IRF3. *Cell* **122**, 669–682 (2005).
18. Gao, D. et al. Cyclic GMP-AMP synthase is an innate immune sensor of HIV and other retroviruses. *Science* **341**, 903–906 (2013).
19. Shalem, O. et al. Genome-scale CRISPR-Cas9 knockout screening in human cells. *Science* **343**, 84–87 (2014).
20. Li, X. D. et al. Pivotal roles of cGAS-cGAMP signaling in antiviral defense and immune adjuvant effects. *Science* **341**, 1390–1394 (2013).
21. Sauer, J. D. et al. The *N*-ethyl-*N*-nitrosourea-induced Goldenticket mouse mutant reveals an essential function of Sting in the in vivo interferon response to *Listeria monocytogenes* and cyclic dinucleotides. *Infect. Immun.* **79**, 688–694 (2011).
22. Yang, H., Wang, H., Ren, J., Chen, Q. & Chen, Z. J. cGAS is essential for cellular senescence. *Proc. Natl Acad. Sci. USA* **114**, E4612–E4620 (2017).
23. Gao, D. et al. Activation of cyclic GMP-AMP synthase by self-DNA causes autoimmune diseases. *Proc. Natl Acad. Sci. USA* **112**, E5699–E5705 (2015).
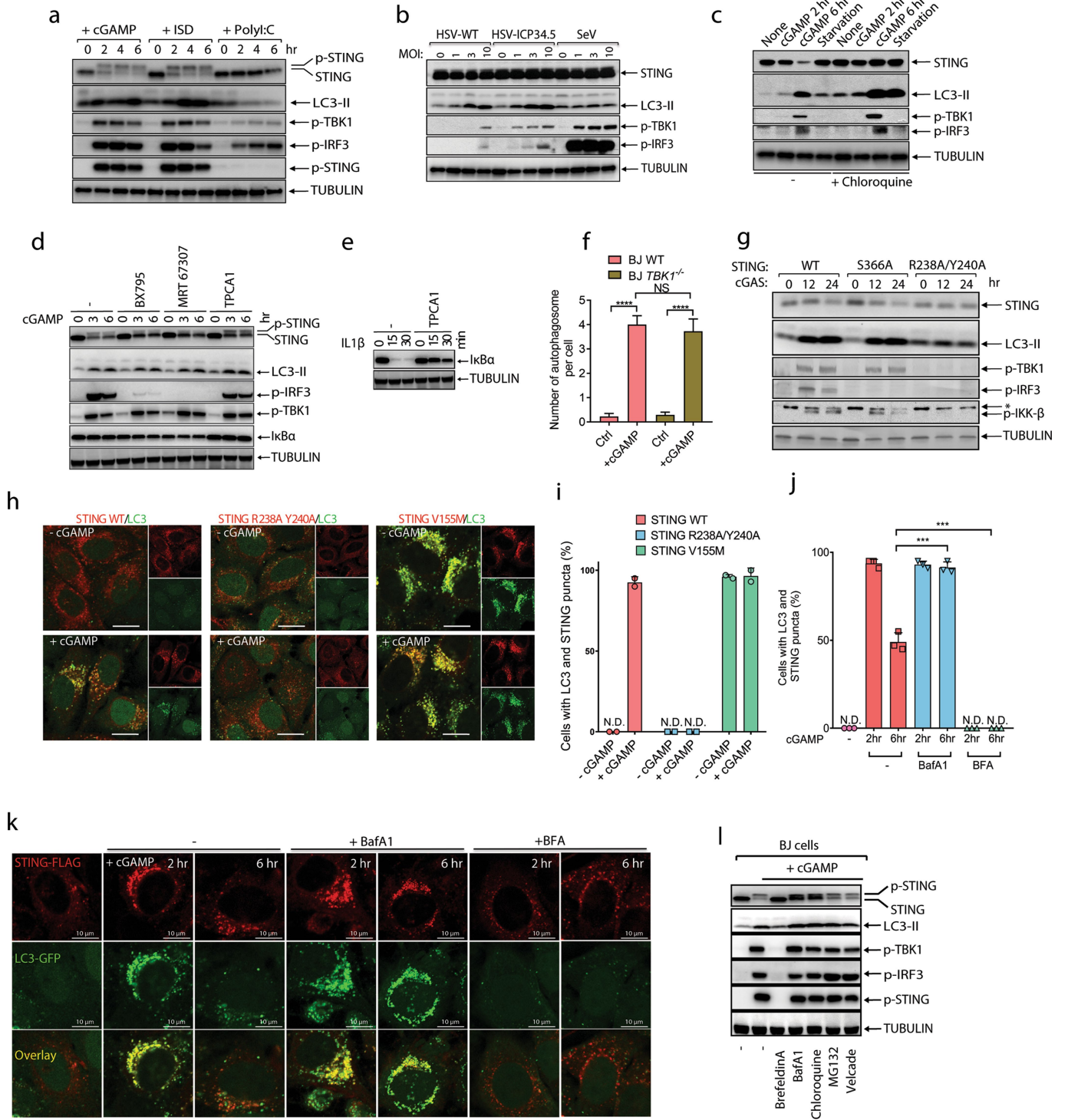
Extended Data Fig. 1 | See next page for caption.

Extended Data Fig. 1 | cGAMP-induced LC3 lipidation requires vesicle trafficking but not TBK1 or IKK. a, DNA and cGAMP, but not RNA, trigger LC3 lipidation. BJ cells were stimulated with cGAMP by digitonin permeabilization or transfected with ISD or poly(I:C). Cell lysates were analysed by immunoblotting with the indicated antibodies. **b**, DNA virus but not RNA virus induces LC3 conversion. BJ cells were infected with wild-type (WT) HSV-1, HSV-1(ΔICP34.5) or Sendai virus (SeV) at the indicated MOI for 6 h followed by immunoblotting. **c**, cGAMP induces STING degradation in the lysosome. HeLa cells that stably express STING–Flag were treated with cGAMP or starved in the presence or absence of chloroquine, followed by immunoblotting. **d**, Inhibition of TBK1 or IKK does not impair LC3 lipidation. Inhibitors of TBK1 (BX-795 or MRT 67307) or IKK (TPCA1) were incubated with BJ cells before stimulation of the cells with cGAMP. Cell lysates were analysed by immunoblotting. **e**, Control experiment showing that TPCA1 inhibits IκBα degradation (by inhibiting IKK). **f**, Quantification of double-membrane autophagosomes in wild-type and $TBK1^{-/-}$ BJ cells. The cells were stimulated with cGAMP as indicated. The number of double-membrane autophagosomes per cell was counted in BJ cells ($n = 13, 12,$ 17, 11). Mean $\pm$ s.e.m. is shown. ****$P < 0.0001$ (two-tailed Student's t-test); NS, not significant (significance level, $\alpha = 0.01$). **g**, STING S366 phosphorylation by TBK1 is essential for IRF3 phosphorylation but not LC3 conversion. HEK293T cells that stably express wild-type or mutant STING(S366A) or STING(R238/Y240A) were transfected with a cGAS expression plasmid followed by immunoblotting. **h**, HeLa cells stably expressing LC3–GFP and different STING mutants (R238A, Y240A or V155M) were stimulated with cGAMP followed by confocal immunofluorescence microscopy. **i**, Quantification of the cells with colocalization of LC3 and STING puncta. The percentage of cells with colocalized LC3 and STING was quantified from 100 cells ($n = 2$). N.D., not detectable. **j**, **k**, HeLa cells that stably express LC3GFP and STING–Flag were treated with bafilomycin A1 (BafA1) or BFA followed by stimulation with cGAMP and confocal immunofluorescence microscopy. The percentage of cells with colocalized LC3 and STING was quantified from 100 cells ($n = 3$, mean $\pm$ s.d., two-tailed Student's t-test). **l**, BJ cells were treated with BFA, lysosome inhibitors (BafA1 or chloroquine) or proteasome inhibitors (MG132 or Velcade) before stimulation with cGAMP. Cell lysates were analysed by immunoblotting.

Extended Data Fig. 2 | Delineation of the STING region (residues 330–334) required for LC3 lipidation. a, Expression plasmids that encode truncated STING mutants were transiently transfected into HEK293T cells for 24 h, followed by stimulation with cGAMP for 4 h. Cell lysates were analysed by immunoblotting. **b**, Expression plasmids of indicated STING truncation leutants were transfected into HeLa LC3–GFP cells for 24 h. The cells were stimulated with cGAMP followed by immunostaining and fluorescence microscopy. **c, d**, Mutations of STING at L333 and R334 impaired LC3 lipidation and TBK1 activation. **c**, Expression plasmids

that encode full-length STING containing the indicated mutations were transiently transfected into HEK293T cells, followed by stimulation with cGAMP. Cell lysates were analysed by immunoblotting. FL, full length. **d**, Indicated STING mutants were transfected and stimulated as described in **c** followed by immunostaining and fluorescence microscopy. **e**, Schematic of functional domains and residues of human (huSTING) and sea anemone STING (nvSTING), highlighting the evolutionary conservation of the cyclic dinucleotide (CDN) binding domain but not the C-terminal activation domain.

a

+2'3'cGAMP

STING-Flag

LC3-II

p-TBK1

p-IRF3

hu-STING FL
nv-STING
hu-STING 1-340
pCDNA3.1

b

hcGAS

nvcGAS

DncV

m/z

c

GFP
NV-cGAS
DNCV
hu-cGAS

d

e

f

g

h

Extended Data Fig. 3 | See next page for caption.

Extended Data Fig. 3 | STING-induced LC3 conversion is a primordial function of the cGAS-STING pathway. a, Sea anemone STING (*Nv*STING) induces LC3 conversion, but not TBK1 activation, in response to 2′3′-cGAMP. HEK293T cells were transfected with expression plasmids encoding full-length human STING (hu-STING), human STING(1–340) or *Nv*STING for 24 h and then treated with 2′3′-cGAMP for 3 h. Cell lysates were analysed by immunoblotting. **b–d**, Sea anemone cGAS (*Nv*cGAS) produces 2′3′-cGAMP. **b**, Expression vectors encoding human cGAS (hu-cGAS), *Nv*cGAS or DncV were transfected into HEK293T cells for 24 h. Small molecules were extracted from cells for analysis of cGAMP isomers by tandem mass spectrometry. Mass spectra of cGAMP from *Nv*cGAS-expressing cells match those from hu-cGAS-expressing cells but not those from DncV-expressing cells. **c**, Similar to **b**, except that the small-molecule extracts were fractionated using a monoQ column, and each fraction was delivered into THP1–ISG luciferase reporter cells for measuring the CDN activity. **d**, CDNs produced by hu-cGAS and *Nv*cGAS, but not that by DncV, is resistant to digestion by RNase T1. Small-molecule extracts from HEK293T cells expressing the indicated CDN synthases were treated with RNase T1 or RNaseT2 or left untreated before delivery into THP1–ISG luciferase reporter cells to measure the CDN activity. Mean ± s.e.m. was shown ($n = 3$) in the group treated with RNase T1. **e**, Domain organization of STING from human (hu), *Danio rerio* (*Dr*) and *Xenopus tropicalis* (*Xt*). **f**, *Xenopus* STING stimulates LC3 lipidation but not IRF3 phosphorylation. HEK293T cells were transfected with expression plasmids for STING–Flag from human, *Danio* or *Xenopus* for 24 h and then stimulated with cGAMP for 1 h. Anti-Flag antibody was used to immunoprecipitate STING from cell lysates followed by immunoblotting with the indicated antibodies. **g**, cGAMP stimulates formation of perinuclear puncta of STING from different species. HeLa cells transiently expressing human, *Danio* or *Xenopus* STING–Flag were stimulated with cGAMP for 3 h. Cells were immunostained with a Flag antibody followed by fluorescence microscopy. **h**, Quantification of the percentage of cells with STING peri-nuclear foci formation. The percentage of cells with STING foci formation was quantified from 100 cells ($n = 2$). All results in this figure are representative of at least two independent experiments.
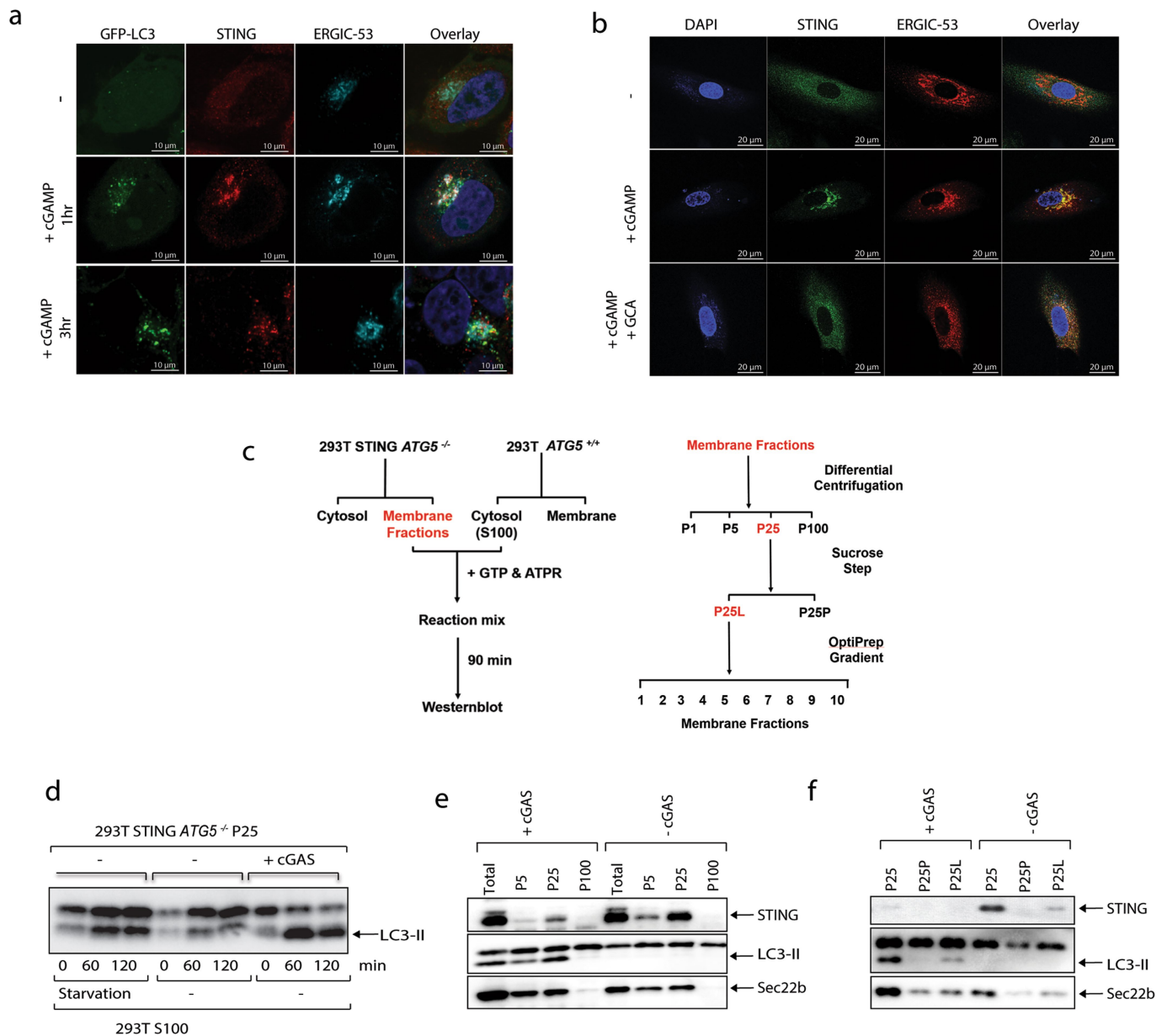
Extended Data Fig. 4 | cGAMP stimulates STING translocation to ERGIC vesicles that promote LC3 lipidation. a, STING colocalizes with the ERGIC and autophagosomes in response to cGAMP stimulation. HeLa cells that stably express GFP–LC3 and STING–Flag were stimulated with cGAMP for the indicated time followed by immunofluorescence microscopy. **b**, STING trafficking to the ERGIC is blocked by GCA. BJ cells were stimulated with cGAMP for 3 h in the presence or absence of GCA. Cells were stained with DAPI or the indicated antibodies and examined by confocal microscopy. **c**, Procedures for in vitro reconstitution of cGAMP-induced LC3 lipidation and membrane fractionation. **d**, $ATG5^{-/-}$ HEK293T cells that stably express STING–Flag were transfected with a cGAS expression plasmid or an empty vector for 24 h.

Membrane pelleted at 25,000g (P25) from these cells was incubated with cytosolic extracts (S100) from starved or untreated 293T cells in the presence of GTP and an ATP regenerating system. After incubation at 30 °C for 90 min, the reaction mixtures were analysed by immunoblotting. **e**, Similar to **c**, except that different organelle membranes enriched by differential centrifugation were prepared and incubated with cytosol (S100) from HEK293T cells to detect LC3 lipidation. **f**, Similar to **c**, except that P25 membranes were further fractionated by sucrose ultracentrifugation to generate P25P (pellet) and P25L (light) and incubated with cytosol (S100) from HEK293T cells to detect LC3 lipidation.
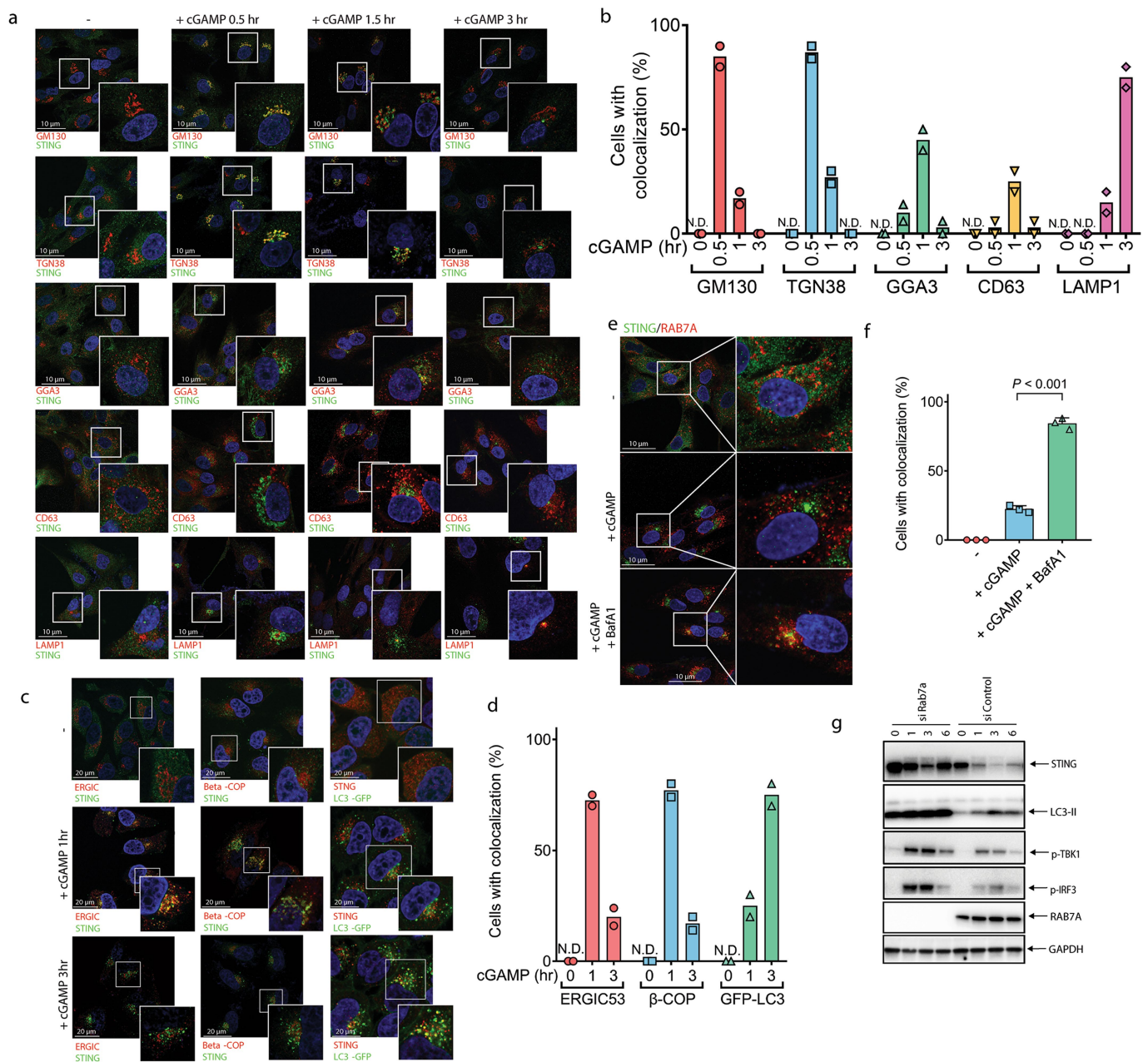
Extended Data Fig. 5 | cGAMP-bound STING traffics through the Golgi and endosomes or the ERGIC and autophagosomes before reaching lysosomes. a, BJ cells were stimulated with cGAMP for the indicated time. Cells were immunostained with a STING antibody together with an antibody against GM130 (*cis*-Golgi), TGN38 (*trans*-Golgi), GGA3 (post-Golgi vesicles), CD63 (late endosomes) or LAMP1 (lysosomes), followed by immunofluorescence microscopy. **b,** Quantification of the percentage of cells in which STING colocalized with different organelle markers in **a**. The percentage was quantified from 50 cells (*n* = 2). All results in this figure are representative of at least two independent experiments. **c,** cGAMP induces trafficking of STING to the ERGIC, COP-I vesicles and LC3 autophagosomes. HeLa cells that stably express STING–Flag and LC3–GFP were stimulated with cGAMP for the indicated time. Cells

were immunostained with antibodies specific for Flag (to detect STING), ERGIC53 (ERGIC) or beta-COP (COP1 vesicles), followed by fluorescence microscopy. **d,** Quantification of the percentage of cells in which STING colocalized with different organelle markers in **c**. The percentage was quantified from 50 cells (*n* = 2). **e,** BJ cells were stimulated with cGAMP in the presence or absence of bafilomycin A1 (BafA1). Cells were immunostained with an antibody specific for STING or RAB7A followed by microscopy. **f,** Quantification of the percentage of cells in which STING colocalized with RAB7A in **e**. The percentage was quantified from 50 cells (*n* = 3, mean ± s.d., two-tailed Student's *t*-test). **g,** BJ cells were transfected with an siRNA targeting *RAB7A* or a control siRNA for three days before stimulation with cGAMP for the indicated time. Cell lysates were analysed by immunoblotting.
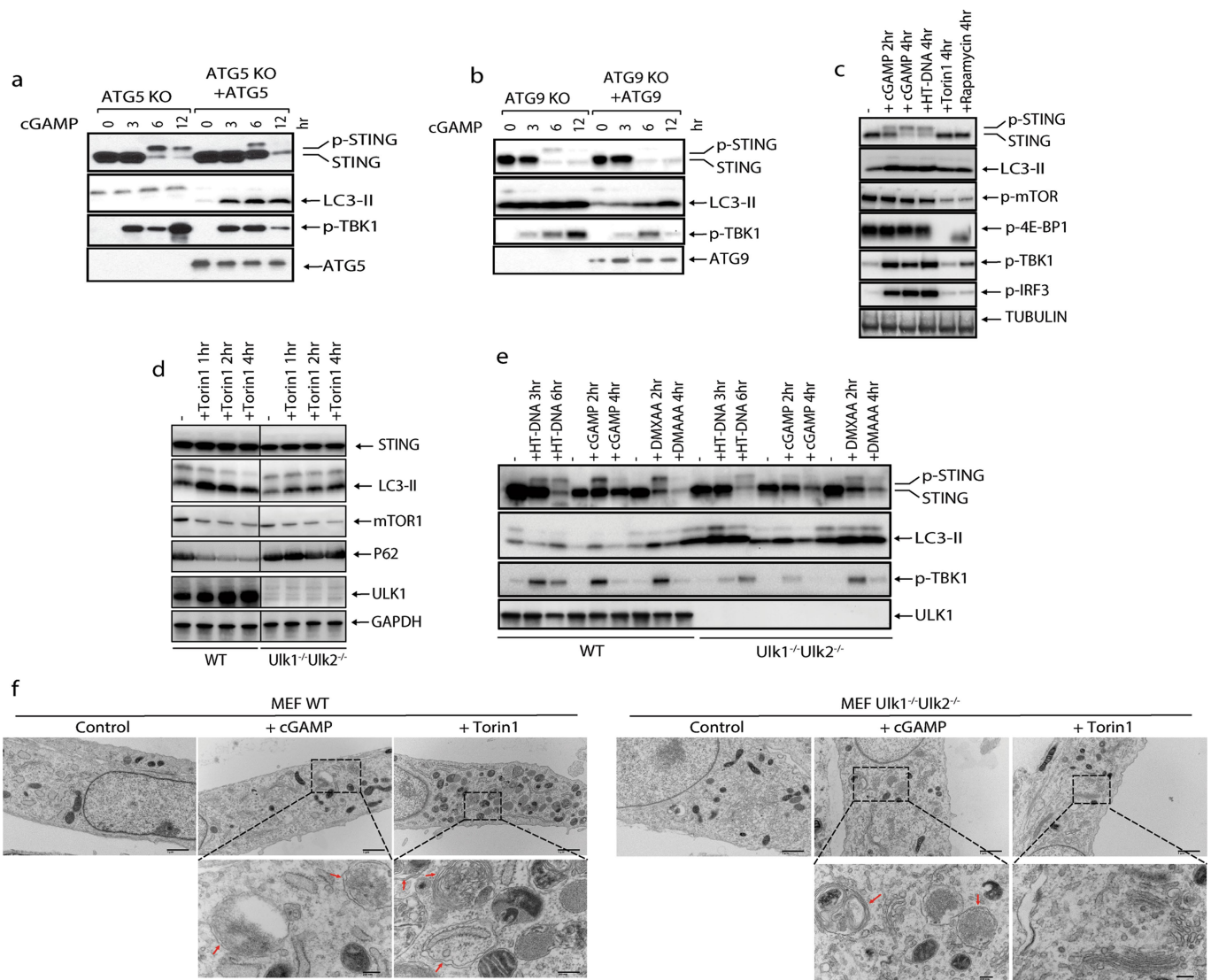
Extended Data Fig. 6 | ULK kinases are dispensable for cGAMP-induced LC3 conversion and autophagosome formation. a, ATG5 is required for LC3 lipidation but dispensable for STING degradation induced by cGAMP. *ATG5*$^{-/-}$ or *ATG5*-reconstituted BJ cells were stimulated with cGAMP for the indicated time followed by immunoblotting of cell lysates. **b**, ATG9 is dispensable for LC3 lipidation and STING degradation. *ATG9*$^{-/-}$ or *ATG9*-reconstituted BJ cells were stimulated with cGAMP for the indicated time followed by immunoblotting of cell lysates. **c**, STING activation does not induce mTOR inhibition. BJ cells were treated with cGAMP, HT-DNA, torin 1 or rapamycin for the indicated time followed by immunoblotting of cell lysates. **d**, Loss of ULK1 and ULK2 impairs LC3 conversion and p62 degradation induced by mTOR inhibition.

Wild-type and *Ulk1*$^{-/-}$*Ulk2*$^{-/-}$ MEF cells were treated with torin 1 at the indicated time followed by immunoblotting of cell lysates. **e**, STING-induced LC3 conversion is independent of ULK1 and ULK2. Wild-type and *Ulk1*$^{-/-}$*Ulk2*$^{-/-}$ MEF cells were treated with cGAMP, HT-DNA or DMXAA for the indicated time followed by immunoblotting of cell lysates. **f**, Electron micrographs of wild-type and *Ulk1*$^{-/-}$*Ulk2*$^{-/-}$ MEF cells stimulated with cGAMP or torin 1. Boxed areas are enlarged to show double-membrane organelles that represent autophagosomes. Red arrows highlight double-membrane characteristic of autophagosomes in stimulated cells. Scale bar, 1 μm (original image), 200 nm (magnified image).
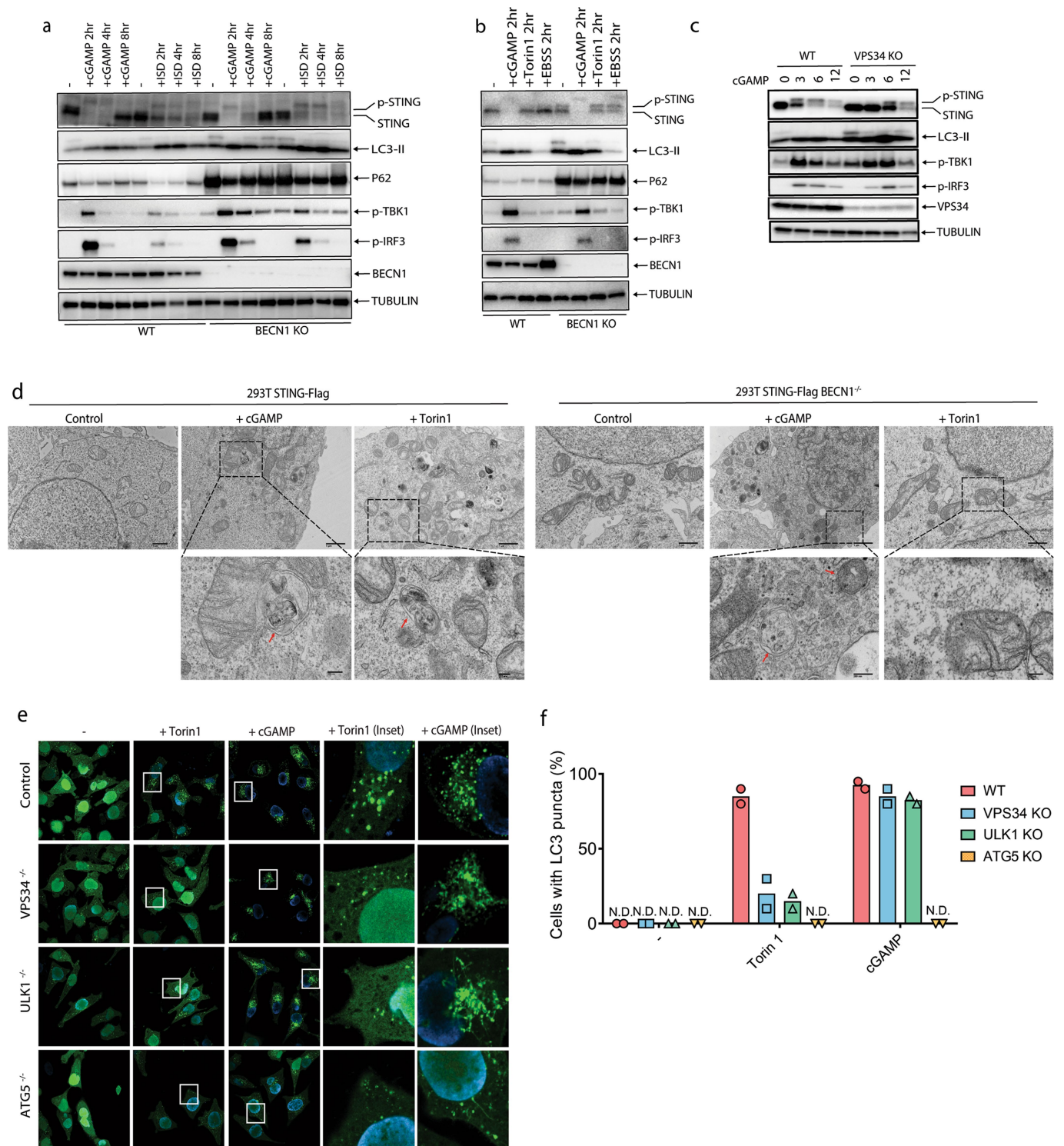
Extended Data Fig. 7 | STING-induced LC3 conversion does not require beclin 1 (BECN1) or VPS34. a, BECN1 is dispensable for LC3 conversion triggered by cGAMP. Wild-type and *BECN1*^{−/−} bone-marrow-derived macrophages were stimulated with cGAMP or HT-DNA at the indicated time followed by immunoblotting of cell lysates. **b**, BECN1 is not essential for LC3 conversion in conventional autophagy. Wild-type and *BECN1*^{−/−} bone-marrow-derived macrophages were stimulated with cGAMP or torin 1 or cultured in EBSS starvation medium at the indicated time, followed by immunoblotting of cell lysates. **c**, VPS34 depletion delayed cGAMP-induced STING degradation but not LC3 lipidation. VPS34-knockout BJ cells were treated with cGAMP for the indicated time followed by immunoblotting of cell lysates. **d**, Electron micrographs of HEK293T

STING–Flag and HEK293T STING–Flag *BECN1*^{−/−} cells, stimulated with cGAMP or torin 1. Boxed areas are enlarged to show double-membrane organelles that represent autophagosomes. Red arrow highlights double-membrane organelles characteristic of autophagosomes in stimulated cells. Scale bar, 1 μm (original image), 200 nm (magnified image). **e**, **f**, ULK1 and VPS34 are essential for LC3 puncta formation induced by torin 1 but not by cGAMP. *ULK1*^{−/−}, *VPS34*^{−/−} or *ATG5*^{−/−} HeLa LC3–GFP cells were treated with torin 1 or cGAMP for the indicated time. LC3–GFP puncta formation was visualized by fluorescence microscopy (**e**) and the percentage of cells with LC3–GFP peri-nuclear foci formation was quantified (**f**). The percentage of cells with LC3–GFP puncta was quantified from 100 cells ($n = 2$).
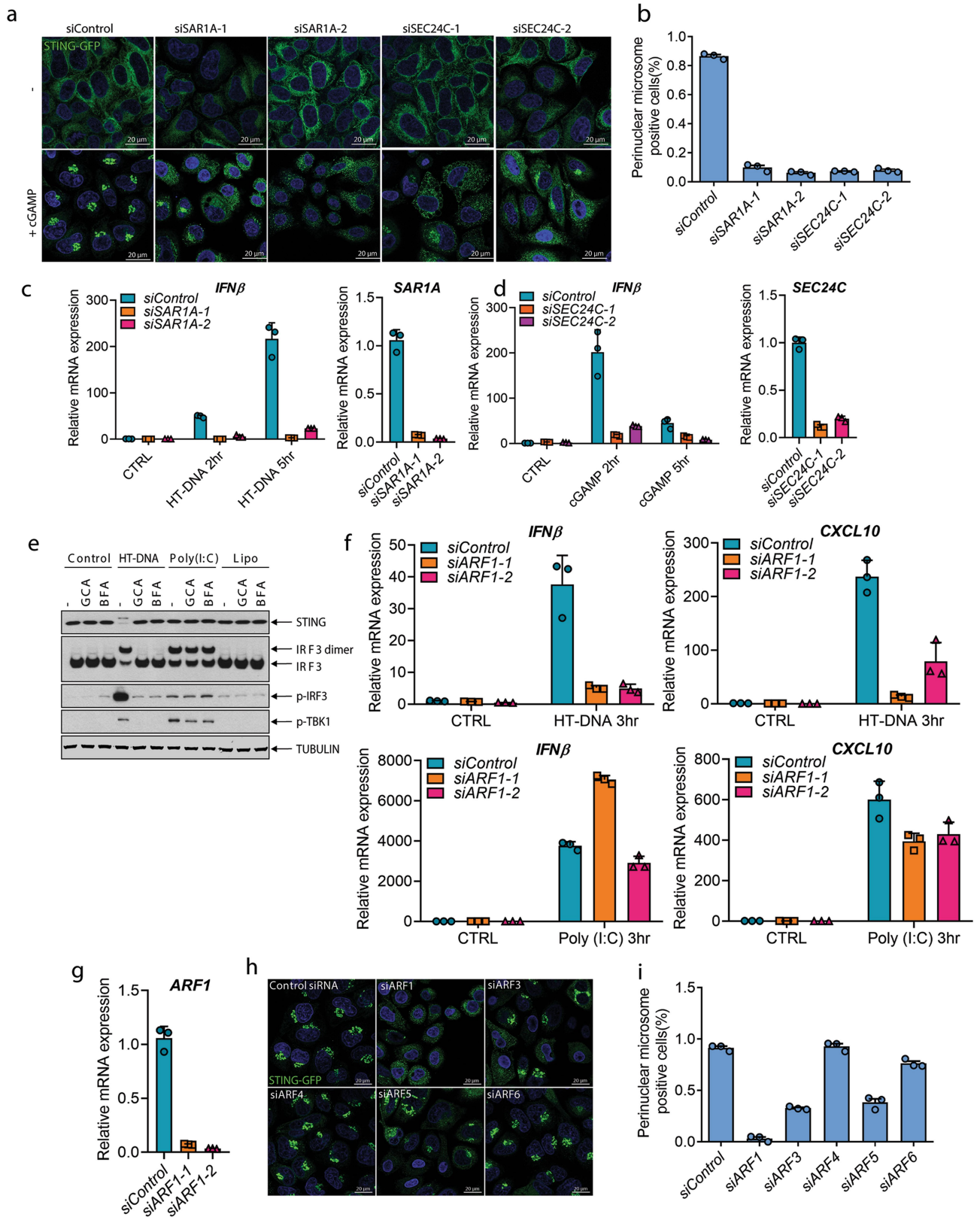
Extended Data Fig. 8 | See next page for caption.

Extended Data Fig. 8 | STING membrane trafficking and signalling requires SAR1A, SEC24C and ARF GTPases. a, **b**, HeLa STING–GFP cells were transfected with siRNAs targeting *SAR1A*, *SEC24C* or luciferase (control) for 3 days before stimulation with cGAMP (75 nM) for 1 h. STING–GFP puncta were detected by confocal microscopy (**a**) and quantified (**b**). The percentage of cells with STING–GFP puncta was quantified from three random fields ($n = 3$, mean ± s.d.). **c**, BJ cells were transfected with siRNAs targeting *SAR1A* for three days before transfection with HT-DNA or poly(I:C) for the indicated time. Total RNA was isolated to measure the expression of indicated genes by RT–qPCR. **d**, Similar to **c**, except that HeLa cells were transfected with siRNAs targeting *SEC24C*, and cells were stimulated with cGAMP or poly(I:C). Mean ± s.d. was shown. Data represent two independent experiments with three replicates. **e**, Membrane trafficking is essential for cytosolic DNA but not RNA signalling. BJ cells were stimulated with BFA or GCA before transfection with HT-DNA or poly(I:C) or Lipofectamine (Lipo) alone. Cell lysates were analysed by native gel (for IRF3 dimerization) or SDS–PAGE followed by immunoblotting with the indicated antibodies. **f**, **g**, BJ cells were transfected with two different siRNAs targeting *ARF1* before transfection with HT-DNA or poly(I:C) for the indicated time. Total RNA was isolated to measure the expression of the indicated genes by RT-qPCR. Mean ± s.d. is shown. Data represent two independent experiments with three replicates. **h**, **i**, HeLa STING–GFP cells were transfected with siRNAs targeting different ARF family members for three days and then stimulated with cGAMP (75 nM) for 1 h. STING–GFP foci were detected by confocal microscopy (**h**) and quantified (**i**). The percentage of cells with STING–GFP puncta was quantified from three random fields ($n = 3$, mean ± s.d.).
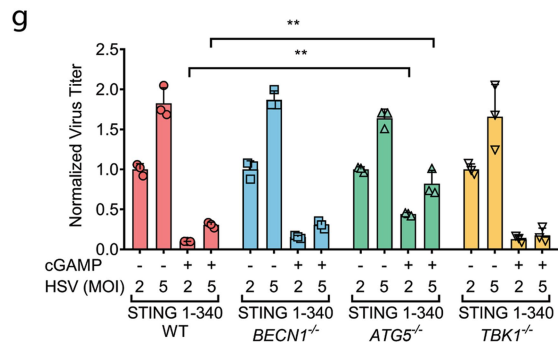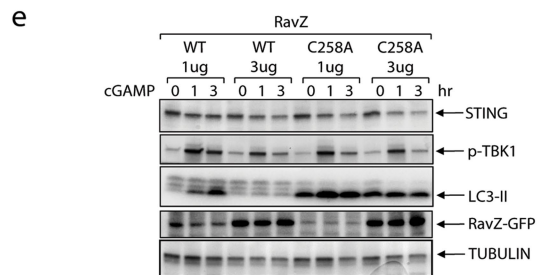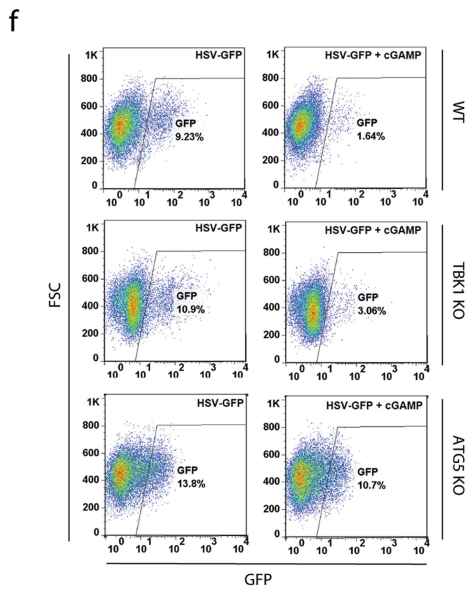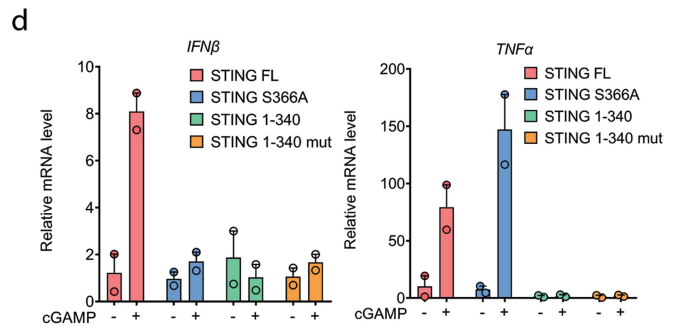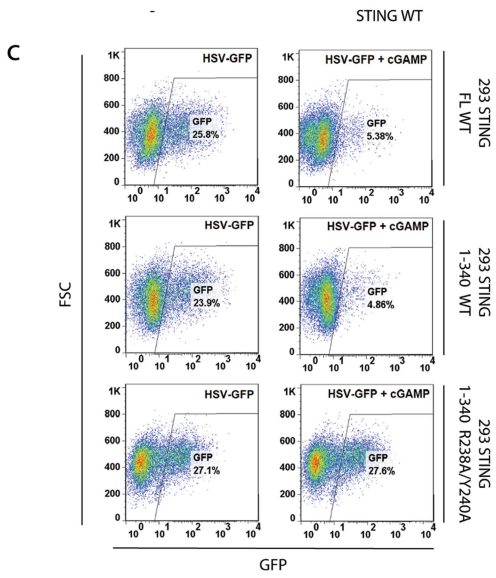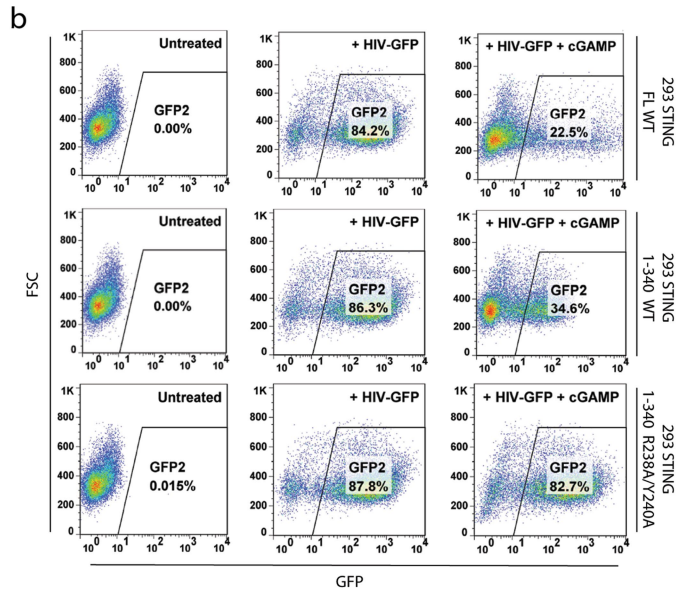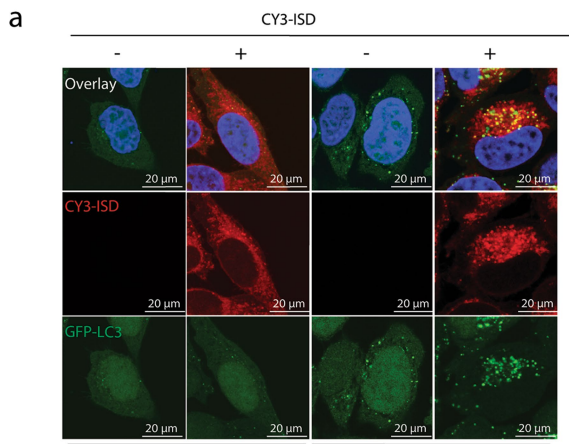
Extended Data Fig. 9 | See next page for caption.

Extended Data Fig. 9 | cGAMP induces anti-viral defence through autophagy. a, Cytosolic DNA colocalizes with LC3 vesicles in STING-expressing cells. Cy3–ISD was delivered into HeLa LC3–GFP cells (lacking endogenous STING) or cells that stably express STING in the presence of PFO, followed by fluorescence microscopy. Single-cell images are shown, representing >90% of the cells under examination. **b, c**, cGAMP-induced activation of STING(1–340) enhances clearance of HIV-1 and HSV-1. HEK293T cells reconstituted with wild-type or mutant STING were stimulated with cGAMP and then infected with the pseudotyped HIV1–GFP virus for 24 h (**b**) or HSV1–GFP for 18 h (**c**). GFP$^+$ cells were analysed by FACS. The results are representative of two independent experiments. **d**, STING(1–340) does not induce IFNβ or TNF. HEK293T cells that stably express full-length STING, STING(S336A), STING(1–340) or STING(1–340, R238A) were stimulated with cGAMP (2 μM) for 8 h and mRNA was extracted for RT–qPCR analysis of expression of the genes for IFNβ or TNF. Representative data are shown from two independent experiments; $n = 2$. Data are presented as mean ± s.d. **e**, RavZ catalyses LC3 deconjugation. HEK293T-STING stable cells were transfected with RavZ expression plasmids (wild-type or C258A mutant) for 36 h and then stimulated with cGAMP for the indicated time. Cell lysates were analysed by immunoblotting with the indicated antibodies. **f**, ATG5 knockout partially reverses cGAMP-mediated repression of HSV-1. ATG5 or TBK1 were knocked out using CRISPR in STING-expressing HEK293T cells. The cells were then infected with HSV–GFP with or without cGAMP treatment. FACS was performed to quantify relative virus GFP intensity in each cell line. **g**, ATG5 deficiency partially abrogated cGAMP-mediated suppression of HSV-1. One of BECN1, ATG5 or TBK1 was knocked out using CRISPR in STING-expressing HEK293T cells. The cells were then infected with HSV-1(ΔICP34.5) with or without cGAMP stimulation. qPCR using HSV-1 primers was performed to quantify relative viral genome equivalent in each cell line; $n = 3$. Data are presented as mean ± s.d. **$P < 0.01$. NS, not significant (two-tailed Student's t-test).
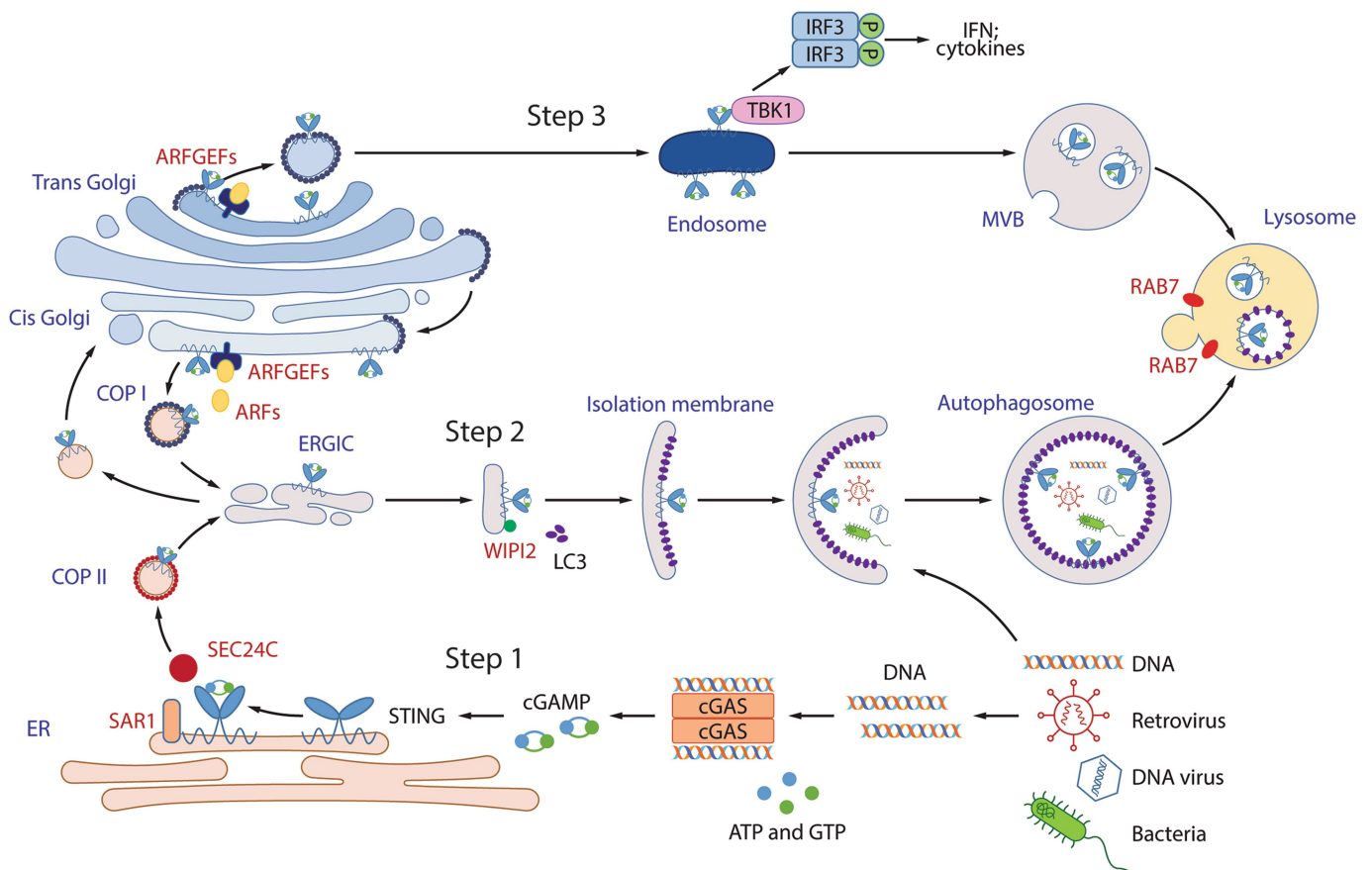
Extended Data Fig. 10 | A model of DNA-induced autophagy and signalling through the cGAS–STING pathway. Step 1, DNA from pathogens or damaged cells activates cGAS to synthesize cGAMP. cGAMP binds to STING and triggers STING translocation from the endoplasmic reticulum to the ERGIC and Golgi in a process that depends on SAR1, SEC24C and ARF family members. Step 2, the ERGIC, which contains cGAMP-bound STING, serves as a membrane source for LC3 recruitment and lipidation through a WIPI2-dependent mechanism. LC3-positive membranes target DNA and pathogens to autophagosomes, which are subsequently fused with lysosomes. Step 3, cGAMP-bound STING can also translocate through the trans-Golgi network and endosomes to lysosomes for degradation via the multi-vesicular body (MVB) pathway. Both the MVB and autophagosome fuse with lysosomes in a process that requires RAB7 GTPase.

Corresponding author(s):   Zhijian J. Chen

Reporting Summary

Nature Research wishes to improve the reproducibility of the work that we publish. This form provides structure for consistency and transparency in reporting. For further information on Nature Research policies, see Authors & Referees and the Editorial Policy Checklist.

Statistical parameters

When statistical analyses are reported, confirm that the following items are present in the relevant location (e.g. figure legend, table legend, main text, or Methods section).

n/a	Confirmed	
☐	☒	The exact sample size (n) for each experimental group/condition, given as a discrete number and unit of measurement
☐	☒	An indication of whether measurements were taken from distinct samples or whether the same sample was measured repeatedly
☐	☒	The statistical test(s) used AND whether they are one- or two-sided *Only common tests should be described solely by name; describe more complex techniques in the Methods section.*
☐	☒	A description of all covariates tested
☐	☒	A description of any assumptions or corrections, such as tests of normality and adjustment for multiple comparisons
☐	☒	A full description of the statistics including central tendency (e.g. means) or other basic estimates (e.g. regression coefficient) AND variation (e.g. standard deviation) or associated estimates of uncertainty (e.g. confidence intervals)
☐	☒	For null hypothesis testing, the test statistic (e.g. F, t, r) with confidence intervals, effect sizes, degrees of freedom and P value noted *Give P values as exact values whenever suitable.*
☒	☐	For Bayesian analysis, information on the choice of priors and Markov chain Monte Carlo settings
☒	☐	For hierarchical and complex designs, identification of the appropriate level for tests and full reporting of outcomes
☐	☒	Estimates of effect sizes (e.g. Cohen's d, Pearson's r), indicating how they were calculated
☐	☒	Clearly defined error bars *State explicitly what error bars represent (e.g. SD, SE, CI)*

Our web collection on statistics for biologists may be useful.

Software and code

Policy information about availability of computer code

Data collection	Images were taken with the built-in softwares of Zeiss LSM 700 microscope and Nikon A1R microscope as detailed in Methods.
Data analysis	Statistical analysis was performed using GraphPad Prism 7. For colocalization analysis, Pearson's correlation coefficient (threshold regression: Costes) was calculated using Coloc 2 plugin of ImageJ.

For manuscripts utilizing custom algorithms or software that are central to the research but not yet described in published literature, software must be made available to editors/reviewers upon request. We strongly encourage code deposition in a community repository (e.g. GitHub). See the Nature Research guidelines for submitting code & software for further information.

Data

Policy information about availability of data

All manuscripts must include a data availability statement. This statement should provide the following information, where applicable:
- Accession codes, unique identifiers, or web links for publicly available datasets
- A list of figures that have associated raw data
- A description of any restrictions on data availability

All important data generated or analyzed during this study are included in this article. Additional supplementary data are available from the corresponding author upon request.

Field-specific reporting

Please select the best fit for your research. If you are not sure, read the appropriate sections before making your selection.

☒ Life sciences   ☐ Behavioural & social sciences   ☐ Ecological, evolutionary & environmental sciences

For a reference copy of the document with all sections, see nature.com/authors/policies/ReportingSummary-flat.pdf

Life sciences study design

All studies must disclose on these points even when the disclosure is negative.

Sample size	For quantification of the number of double-membrane autophagosomes per cell , 25–35 cells were randomly taken throughout the slide of each sample. For quantification of STING foci formation, 10-20 non-overlapping whole-field images were randomly taken throughout the slide of each sample and the number of those with phenotype of interest was recorded from 100 cells. This process was repeated for a total of three times. The sample sizes were selected based on power analysis of results from preliminary experiments, which shows that the sample sizes are not only sufficient to obtain desirable significance level (< 0.01) and power (>90%), but also able to generate highly reproducible results with biological replicates.
Data exclusions	No data was excluded.
Replication	All experiments were confirmed with multiple biological replicates as detailed in figure legends, and the representative results are shown.
Randomization	For quantification of percentages of cells with phenotype of interest, images were randomly taken throughout the slide of each sample using DAPI channel to avoid bias in selection of cells with particular phenotypes, before other channels were used for imaging.
Blinding	Immunoblots arrays were exposed with the same settings without the investigators knowing the order of the samples. They were identified later with markers assigned to them. Images were collected with randomization described above and a code number was assigned for each group. The investigators performed the quantification before the identities of the groups were added to the samples according to the code numbers.

Reporting for specific materials, systems and methods

Materials & experimental systems

n/a	Involved in the study
☒	☐ Unique biological materials
☐	☒ Antibodies
☐	☒ Eukaryotic cell lines
☒	☐ Palaeontology
☐	☒ Animals and other organisms
☒	☐ Human research participants

Methods

n/a	Involved in the study
☒	☐ ChIP-seq
☐	☒ Flow cytometry
☒	☐ MRI-based neuroimaging

Antibodies

Antibodies used	Rabbit antibodies against human STING(13647), p-IRF3(Ser396)(#947), p-TBK1(Ser172)(5483), p-IKKβ(Ser177)(2078), ATG5(12994), ATG9(13509), Beclin1(3738), calreticulin(12238), and GAPDH(2118) were from Cell Signaling. Rabbit Polyclonal antibody against mouse STING(19851-1-AP) was from Proteintech. Mouse antibody against STING(MAB7169) was purchased from R&D Systems; rabbit antibodies against human IRF3(33641), TGN38(166594), and ARF1(sc-53168) and mouse antibody against CD63(5275) were from Santa Cruz Biotechnology; rabbit antibody against LC3(NB100-2220) was from Novus Biologicals; mouse antibodies against P62(610833) and GGA3(612311) were from BD Transduction Laboratories; mouse antibody against ERGIC-53 (ALX-804-602-C100) was from Axxora; rabbit antibody against Sec22b(186003) was from Synaptic Systems; mouse antibody against Flag tag(F3165), rabbit antibodies against ERGIC53(E1031), beta-tubulin(T4026) and anti-Flag (M2)-conjugated agarose(A2220) and anti-HA–conjugated agarose(E6779) were from Sigma; HA antibody was from Covance; rabbit antibodies against GBF1(86071), LAMP2(25631), and Giantin(24586) were from Abcam; rabbit antibody against beta-COP(PA1-061) was from Thermo Fisher; rabbit antibodies against ARFGEF1(A300-998A), ARFGEF2(A301-004A), and SEC24C(A304-760A) were from Bethyl Laboratories. All primary antibodies were used in 1:1,000 dilution. Alexa Fluor secondary antibodies (488, 568, and 633) were used in 1:200 dilution.
Validation	All the commercial antibodies have been verified by the manufacturers according to the immunoblots and/or images on their websites. Data are provided per quality assurance by each supplier. The home made STING antibody was verified in this paper

(Tanaka et al. Sci Signal. 2012 Mar 6;5(214):ra20).

Eukaryotic cell lines

Policy information about cell lines

Cell line source(s)	Cell lines including HEK293T,L929, HeLa, BJ and THP1 cells were obtained from ATCC (https://www.atcc.org/).The Beclin 1 knockout BMDM is from LysM-Cre+Beclin 1flox/flox mice and the control BMDM is from Beclin 1flox/flox mice. WT cGas KO and Sting KO MEF cells were generated from E13.5 embryos of WT and mutant mice under normal culture conditions. Ulk1-/-Ulk2-/- (DKO) MEF cells were from Sigma (14050803-1VL).
Authentication	The cell lines used in this study were verified by ATCC (https://www.atcc.org/) and were constantly monitored for contamination from other cell lines. None of the cell lines have been authenticated. The webpages of ATCC describe the authentication methods for these cell lines: HEK293T: https://www.atcc.org/en/Products/All/CRL-3216.aspx HeLa: https://www.atcc.org/Products/All/CCL-2.aspx L929: https://www.atcc.org/products/all/CCL-1.aspx BJ: https://www.atcc.org/products/all/CRL-4001.aspx THP1: https://www.atcc.org/products/all/TIB-202.aspx
Mycoplasma contamination	The cell lines used in this study were free of mycoplasma contamination based on the results of e-Myco Mycoplasma PCR Detection Kit (Bulldog Bio) and were regularly maintained with Normocin (antimicrobial reagent against mycoplasma, bacteria and fungi) (InvivoGen).
Commonly misidentified lines (See ICLAC register)	No commonly misidentified cell lines were used.

Animals and other organisms

Policy information about studies involving animals; ARRIVE guidelines recommended for reporting animal research

Laboratory animals	cGas-/- mice were generated as described previously(Li et al. Science 2013, 341, 1390-1394). Sting gt/gt mice were from the Jackson laboratory (Stock No: 017537). All the mouse are on C57BL/6 background and used at 6-8 of weeks. All colonies were housed and bred in individually ventilated cages in the animal facility of UTSW.
Wild animals	The study did not involve wild animals.
Field-collected samples	The study did not involve field-collected samples.

Flow Cytometry

Plots

Confirm that:

☒ The axis labels state the marker and fluorochrome used (e.g. CD4-FITC).

☒ The axis scales are clearly visible. Include numbers along axes only for bottom left plot of group (a 'group' is an analysis of identical markers).

☒ All plots are contour plots with outliers or pseudocolor plots.

☒ A numerical value for number of cells or percentage (with statistics) is provided.

Methodology

Sample preparation	Cells were washed in FACS buffer (PBS, 1% BSA), fixed with 2% paraformaldehyde
Instrument	D FACSCalibur (BD Biosciences)
Software	analyzed on B. Data analysis was performed using FlowJo software.
Cell population abundance	20000
Gating strategy	*Describe the gating strategy used for all relevant experiments, specifying the preliminary FSC/SSC gates of the starting cell population, indicating where boundaries between "positive" and "negative" staining cell populations are defined.*

☒ Tick this box to confirm that a figure exemplifying the gating strategy is provided in the Supplementary Information.